Hypoxia-inducible factor 2α drives nonalcoholic fatty liver progression by triggering hepatocyte release of histidine rich glycoprotein.

Hypoxia-inducible factor 2α drives nonalcoholic fatty liver progression by triggering hepatocyte release of histidine rich glycoprotein

Elisabetta Morello[1]*, **Salvatore Sutti**[2,3]*, Beatrice Foglia[1], Erica Novo[1], Stefania Cannito[1], Claudia Bocca[1], Martina Rajsky[1], Stefania Bruzzì[3], Maria Lorena Abate[2], Chiara Rosso[2], Cristina Bozzola[3], Ezio David[4], Elisabetta Bugianesi[2], Emanuele Albano[3], Maurizio Parola[1§]

[1]Dept. Clinical and Biological Sciences, University of Torino, Italy.

[2]Dept. Medical Sciences, University of Torino, Italy.

[3]Dept. Health Sciences and Interdisciplinary Research Center for Autoimmune Diseases, University Amedeo Avogadro of East Piedmont, Novara, Italy.

[4]Pathology Unit, S. Giovanni Battista Hospital, Torino.

*These Authors contributed equally to this study

[§]Corresponding Author /Contact Information: Maurizio Parola – maurizio.parola@unito.it

Author names

Elisabetta Morello elisabetta.morello@unito.it

Salvatore Sutti salvatore.sutti@med.uniupo.it

Beatrice Foglia beatrice.foglia@unito.it

Stefania Cannito stefania.canito@unito.it

Erica Novo erica.novo@unito.it

Claudia Bocca claudia.bocca@unito.it

Martina Rajsky rajsky.martina@gmail.com

Stefania Bruzzì stefania.bruzzi@med.uniupo.it

Maria Lorena Abate marialorena.abate@unito.it

Chiara Rosso chiara.rosso@unito.it

Cristina Bozzola cristina.bozzola@med.uniupo.it

Ezio David ezio.david@unito.it

Elisabetta Bugianesi elisabetta.bugianesi@unito.it

Emanuele Albano emanuele.albano@med.uniupo.it

Maurizio Parola maurizio.parola@unito.it

Conflict of Interest: none declared

Keywords: HIF-2α, NAFLD progression, NAFLD murine model, histidine rich glycoprotein,

Word Count: 5701 words (including references)

Number of Figures/Tables: 7 Figures + 9 Supplementary Figures, 2 Supplementary Tables

FOOTNOTE PAGE

Contact Information: Prof. Maurizio Parola, Dept. Clinical and Biological Sciences, Unit of Experimental Medicine and Clinical Pathology, University of Torino

Corso Raffaello 30, 10125 Torino, Italy.

Phone +39-011-6707772 Fax +39-011-6707753

e-mail maurizio.parola@unito.it

List of abbreviations. NAFLD, nonalcoholic fatty liver disease; CLD, chronic liver disease; NASH, nonalcoholic steatohepatitis; HCC, hepatocellular carcinoma; HIFs, Hypoxia-inducible factors; HIF-1α, hypoxia-inducible factor-1α; HIF-2α, hypoxia-inducible factor-2α; HIF-1β, hypoxia-inducible factor-1β; ROS, reactive oxygen species; HRGP, histidine-rich glycoprotein; MCD diet, methionine/choline deficient diet; CDDA diet, choline-deficient L-aminoacid-defined diet; MCS diet, methionine/choline sufficient diet; CSAA diet, choline sufficient L-aminoacid-defined diet; ALT, alanine aminotransferase; Q-PCR, quantitative real-time polymerase chain reaction; TNFα, tumour necrosis factor-α; IL, interleukin; CCL2, C-C-motif chemokine ligand 2; CXCL10, C-X-C-motif chemokine ligand 10; IHC, Immunohistochemistry; VEGF, vascular-endothelial growth factor; TGFβ1, transforming growth factor β1; α-SMA, α-smooth muscle actin.

Financial Support: This study has been funded by: i) European Union's Horizon 2020 research and innovation programme under grant agreement No. 634413 for the project EPoS (Elucidating Pathways of Steatohepatitis) (to EB); ii) Associazione Italiana per la Ricerca sul Cancro (AIRC, Milano, Italy), grant n. 15274 (to MP); iii) The CariPLO Foundation (Milan, Italy), grant n. 2011-0470 (to EA and MP); iv) The University of Torino (Torino, Italy), (to EN and MP). The funders had no role in the study design, data collection and analysis, decision to publish, or preparation of the manuscript.

ABSTRACT

Mechanisms underlying progression of non-alcoholic fatty liver disease (NAFLD) are still incompletely characterized. Hypoxia and hypoxia inducible factors (HIFs) have been implicated in the pathogenesis of chronic liver diseases but the actual role of HIF-2α in the evolution of NAFLD has never been investigated in detail. In this study, we show that HIF-2α is selectively overexpressed in the cytosol and the nuclei of hepatocytes in a very high percentage (> 90%) of liver biopsies from a cohort of NAFLD patients at different stage of the disease evolution. Similar features were also observed in mice with steatohepatitis induced by feeding a methionine/choline-deficient (MCD) diet. Experiments performed in mice carrying hepatocyte-specific deletion of HIF-2α and related control littermates fed with either choline-deficient L-amino acid-refined (CDAA) or MCD diets showed that HIF-2α deletion ameliorated the evolution of NAFLD by decreasing parenchymal injury, fatty liver, lobular inflammation and the development of liver fibrosis. The improvement in NAFLD progression in HIF-2α deficient mice was related to a selective down-regulation in the hepatocyte production of Histidine-Rich Glycoprotein (HRGP), recently proposed to sustain macrophage M1 polarization. In vitro experiments confirmed that the up-regulation of hepatocyte HRGP expression was hypoxia- and HIF-2α-dependent. Finally, analyses performed on specimens from NAFLD patients indicated that HRGP was overexpressed in all patients showing hepatocyte nuclear staining for HIF-2α and revealed a significant positive correlation between HIF-2α and HRGP liver transcripts levels in these patients.

Conclusions: These results indicate that hepatocyte HIF-2α activation is a key feature in both human and experimental NAFLD and significantly contributes to the disease progression through the up-regulation of HRGP production.

Abstract word count: 263

Non-alcoholic fatty liver disease (NAFLD), regarded as the hepatic manifestation of the metabolic syndrome, is becoming the most frequent chronic liver disease (CLD) worldwide with a prevalence up to 20-30% in the general population and even higher among obese individuals and/or patients affected by Type II diabetes mellitus.[1-6] NAFLD can evolve (20-30% of patients) in non-alcoholic steatohepatitis (NASH), characterized by hepatocyte injury and lobular inflammation that, in turn, can progress to fibrosis, cirrhosis and hepatocellular carcinoma (HCC), but at present mechanisms underlying NAFLD progression are still incompletely characterized and no validated therapy is currently available.[1,4-7]

Literature data suggest that hepatic hypoxia can have a role in CLD progression and HCC development by sustaining both angiogenesis and fibrogenesis as well as, possibly, also inflammatory response and autophagy, with hepatic myofibroblasts being able to both respond to hypoxia and to act in pro-angiogenic way. [8-11] The cellular response to hypoxia is mainly operated by hypoxia-inducible factors (HIFs), evolutionary conserved heterodimeric transcriptional factors consisting of an oxygen-sensitive α-subunit (HIF-1α or HIF-2α) and a stable, constitutively expressed, β-subunit (HIF-1β).[12-14] So far, data concerning the role of hypoxia and HIFs in NAFLD are quite limited [10] but morphological evidence indicate that liver hypoxia develops in parallel with NAFLD-mediated steatosis, particularly in peri-venous areas, similarly to what described for ethanol-induced fatty liver. [15,16] Nonetheless, HIFs can be regulated also by oxygen-independent mechanisms such as mitochondrial dysfunction, reactive oxygen species (ROS) generation and endoplasmic reticulum stress. [8-14] On their turn, HIF-1α and HIF-2α can modulate the cellular adaptive responses to hypoxia by up-regulating either common or, more often, distinct and non-overlapping transcriptional programs. For instance, HIF-1α promotes glucose consumption and glycolysis while lipid storage is mainly regulated by HIF-2α. [12-14] These actions on cell metabolism are potentially relevant for the pathogenesis of NAFLD since hypoxic conditions have been

reported to stimulate lipid storage and inhibit lipid catabolism through β-oxidation.[10,12,13,17] Although both HIF-1α and HIF-2α affect lipid metabolism, experimental studies indicate that HIF-2α activation leads to fatty liver by both up-regulating genes involved in fatty acid synthesis/uptake and lipid storage and down-regulating those involved in fatty acid catabolism.[18,19] HIF-2α activation has also been related to an early increase in the transcription of pro-inflammatory cytokines and of genes involved in fibrogenesis. [19] However, these data have been obtained in mice carrying multiple genetic manipulations in the absence of liver injury [18,19] or in the frame of a short protocol (2 weeks) of ethanol administration using Lieber-De Carli liquid diet, all conditions that do not reproduce the conditions occurring in NAFLD.[19] At present, relevant human data about the role of HIF-2α in fatty liver development and NAFLD progression are lacking. On the other hand, despite HIF-1α appears to sustain fibrogenesis in the bile duct ligation experimental model of CLD, [20] other studies designed to specifically target hepatocyte HIF-1α in experimental models of alcoholic or NAFLD-related steatosis and progression have led to conflicting results. [21-24]

In this study, the analysis of liver biopsies from a cohort of NAFLD patients and the induction of experimental NAFLD with two different dietary protocols in mice carrying hepatocyte-specific deletion of HIF-2α provide evidence indicating that HIF-2α plays a critical role in NAFLD progression by up-regulating hepatocyte expression of histidine-rich glycoprotein (HRGP).

Material & Methods

Human Subjects

The study on NAFLD patients was approved by the ethics' committee of the Azienda Ospedaliera Universitaria Città della Salute, Torino, Italy. For this study we analyzed liver biopsies from NAFLD patients (n=27) ranging from early disease (staged F0-F1) to more advanced conditions of fibrosis (staged F2-F3) or cirrhosis (F4) and referring to the Division of Gastro-Hepatology of the University of Turin. All samples were collected at the time of first diagnosis. Patients were characterized by anthropometric, clinical and biochemical data and liver biopsies were evaluated for the severity of steatohepatitis and fibrosis according to Kleiner et al. [25] All subjects gave informed consent to the analysis and the study protocol, conformed to the ethical guidelines of the 1975 Declaration of Helsinki, was planned according to the guide-lines of the local ethical committee. The clinical and biochemical features of the patients are reported in Supplementary Table 1. Control human liver tissue (n=5), as defined for normal histological structures in hematoxylin and eosin (H&E) sections and the absence of inflammation in the portal tract and parenchyma, was obtained from diagnostic biopsies or from resection samples taken at a distance of more than 5 cm from the border of liver metastasis of colon carcinoma.

Animal experimentation

Mice carrying a hepatocyte-specific deletion of HIF-2α (hHIF-2α $^{-/-}$) were obtained by breeding HIF-2α $^{fl/fl}$ C57BL/6 mice with mice on the same genetic background expressing the Cre-recombinase under the control of the Albumin promoter (Alb/Cre $^{+/+}$ mice) (Jackson Laboratories, Bar Harbor, Maine, USA). Eight weeks old male hHIF-2α $^{-/-}$ mice and related control sibling littermates not carrying HIF-2α deletion, were fed with either methionine/choline deficient (MCD) diet for 4 or 8 weeks or choline-deficient L-aminoacid-defined (CDDA) diet (Laboratorio Dottori Piccioni, Gessate,

Italy) for 12 and 24 weeks.[26,27] Control littermates received the corresponding methionine/choline or choline sufficient diets (MCS or CSAA, respectively). In preliminary experiments eight-week-old normal C57BL/6 mice were fed on the MCD diet or to MCS control diet for 4 and 8 weeks. The experiments complied with national ethical guidelines for animal experimentation and the experimental protocols were approved by the Italian Ministry of Health.

Biochemical Analyses.

Plasma alanine aminotransferase (ALT) and liver triglycerides were determined by spectrometric kits supplied by Radim S.p.A. (Pomezia, Italy) and Sigma Diagnostics (Milano, Italy), respectively. Circulating IL-12 was evaluated by commercial ELISA kits supplied by Peprotech (Milano, Italy).

Immunohistochemistry, Sirius Red staining and histo-morphometric analysis.

Immunohistochemistry,[28,29] Picro-Sirius Red staining and histomorphometric analysis [30,31] were performed on paraffin-embedded human liver biopsies and/or murine liver specimens as previously reported. More details are in the Supplementary material.

Quantitative real-time PCR (Q-PCR).

RNA extraction, complementary DNA synthesis, quantitative real-time PCR (Q-PCR) reactions were performed on human and murine liver speciments as previously described. [28-30] mRNA levels were measured by Q-PCR, using the SYBR® green method as described. [28-30] More details and oligonucleotide sequences of primers used for Q-PCR are available in the Supplementary Material section. The murine transcripts for tumour necrosis factor-α (TNFα), CD11b, interleukin (IL) -12p40, C-C-motif chemokine ligand 2 (CCL2), C-X-C-motif chemokine ligand 10 (CXCL10), HRGP, β-actin liver RNA were retro-transcribed with High Capacity cDNA Reverse Transcription Kit (Applied Biosystems Italia, Monza, Italy). Q-PCR for these transcripts was performed in a Techne TC-312

thermacycler (TecneInc, Burlington NJ, USA) using TaqMan Gene Expression Master Mix and TaqMan Gene Expression probes for indicated murine genes (Applied Biosystems Italia, Monza, Italy) as previously described. [26,31] Human sample analysis was performed using SsoFast™ EvaGreen® Supermix (Biorad, Hercules, CA, USA) following manufacturer's instructions.

*Intrahepatic mononucleated cell isolation and flow cytometry analysis***.**

Hepatic mononucleated cells were isolated from the livers of naive and CDAA-fed mice and purified on a density gradient (Lympholyte®-M, Cedarlane Laboratoires Ltd. Burlington, Canada) as described. [31] Cells were washed with Hank's medium and incubated 30 min with de-complemented mouse serum to block unspecific immunoglobulin binding. The cells were then stained with fluorochrome-conjugated antibodies for CD45, CD11b, Ly6C, (eBiosciences, San Diego CA, USA), F4-80 (Invitrogen, Abingdon, UK) and analyzed with a AttuneTM NxT acoustic focusing cytometer (Thermo Fischer Scientific, , Waltham, MS, USA) following prior gating for CD45 and the absence of cell aggregates. Intracellular staining for IL-12 was performed using a specific fluorochrome-conjugated antibody (eBiosciences, San Diego CA, USA).

In vitro experiments and Western Blot analysis

In vitro experiments in this study were performed in normal HepG2 cells (American Type Culture Collection, USA) as well as in cells stably transfected in order to overexpress HIF-2α in either normoxic or hypoxic conditions, as previously reported. [28] Western blot analysis was performed on total cell or tissue lysates as previously described. [28,30] More details on in vitro studies and WB analysis are available in Supplementary material.

Data analysis and statistical calculations.

Statistical analyses were performed by SPSS statistical software (SPSS Inc. Chicago IL, USA) using one-way ANOVA test with Tukey's correction for multiple comparisons or Kruskal-Wallis test for non-parametric values. Significance was taken at the 5% level. Normality distribution was preliminary assessed by the Kolmogorov-Smirnov algorithm.

Results

HIF-2α is overexpressed in human and murine hepatocytes in NAFLD-related liver specimens

Immunohistochemistry (IHC) analysis of liver biopsies from a cohort of well characterized NAFLD patients (n= 27, see Supplementary Table 1 for patient characterization) at different stages of the disease evolution showed a well evident increase of HIF-2α immune-staining as compared to undamaged liver samples (n=5) from patients undergoing resection for hepatic metastasis of colon carcinoma. In the majority of NAFLD patients (25 out of 27; 92%) HIF-2α positivity was detectable almost exclusively in hepatocytes (Figure 1A,B) and involved both the cytoplasm and the nuclei, although the number of positive nuclei varied within patients and also in different areas of the same biopsy (Figure 1A). The nuclei of non-parenchymal cells, mainly inflammatory cells or myofibroblast-like cells in fibrotic septa, were essentially negative for HIF-2α. Occasionally, HIF-2α staining was observed in portal/periportal cholangiocytes, particularly in subjects with advanced fibrosis. Semi-quantitative assessment of HIF-2α positive hepatocyte nuclei confirmed a significant increase among NAFLD patients irrespectively from the stage of the disease (Figure 1B). These findings were reproduced in a rodent model of NAFLD-related liver fibrosis based on mice feeding with a methionine and choline-deficient (MCD) diet up to 8 weeks (Supplementary Figure 1A,B). In fact, while in control mice HIF-2α staining was only detected in the cytoplasm of hepatocytes closely surrounding centrilobular veins (Supplementary Figure 1A), extensive HIF-2α positivity was evident in liver sections from mice receiving the MCD diet (Supplementary Figure 1B). In these animals Q-PCR analyses confirmed that both HIF-2α as well HIF-1α transcripts were up-regulated in mice with NAFLD, but only those of HIF-2α paralleled the disease progression (Supplementary Figure 1 C-F).

Hepatocyte-specific deletion of HIF-2α improves NAFLD-associated liver injury, steatosis, inflammatory response and fibrosis

Based on previous data, we seek to evaluate whether HIF-2α deletion in hepatocytes might modify NAFLD evolution. To this aim, progressive NAFLD was induced in mice carrying hepatocyte-specific deletion of HIF-2α (hHIF-2α$^{-/-}$ mice) as well as related control littermates by two dietary protocols using a MCD diet, administered for 4 and 8 weeks and a choline-deficient L-aminoacid-defined (CDDA) diet, administered for 12 and 24 weeks. In preliminary experiments, we first checked for effective HIF-2α depletion in the livers of hHIF-2α$^{-/-}$ mice receiving the MCD diet. As reported in Supplementary Figure 2A-C, Q-PCR analysis revealed a very significant down-regulation of liver HIF-2α transcripts in hHIF-2α$^{-/-}$ mice as compared to control littermates, whereas HIF-1α and vascular-endothelial growth factor (VEGF) transcript levels were not affected. HIF-2α deletion was also confirmed at protein levels by western blotting of total liver proteins (Supplementary Figure 2D).

Interestingly, in hHIF-2α$^{-/-}$ mice receiving the MCD diet for 4 weeks the severity of steatohepatitis as evaluated by histology, alanine aminotransferase (ALT) release and by hepatic triglycerides accumulation was significantly lower than in HIF-2α sufficient animals (Figure 2 A-C). The extent of lobular inflammation and the hepatic expression of inflammatory markers TNF-α, CD11b, and CCL2 were also decreased in hHIF-2α$^{-/-}$ mice receiving the MCD diet (Figure 2D). On the same line, using CDAA fed mice we observed that the deletion of hepatocyte HIF-2α (which was confirmed also by means of IHC in these mice vs control littermates, see Suppl. Figure 3) slowed-down the time-dependent progression of NAFLD (Figure 3A,B,E) without affecting the gain in body weight and the development of insulin resistance (Figure 3C,D). In this experimental model, hHIF-2α$^{-/-}$ mice also showed less liver fibrosis at both 12 and 24 weeks, as evidenced by Sirius Red staining (Figure 4A,B). This paralleled a decrease in hepatic transcript for transforming growth factor β1 (TGFβ1),

α-smooth muscle actin (α-SMA) and collagen 1A1 (Figure 4C), as well as in the number of α-SMA positive myofibroblasts detected by immunohistochemistry (Figure 4D). Remarkably, the protection from fibrosis was also evident in hHIF-2α$^{-/-}$ mice receiving the MCD diet up to 8 weeks as compared to control HIF-2α sufficient littermates (Suppl. Figure 4A-D).

Hepatocyte-specific deletion of HIF-2α prevents the progression of experimental NAFLD by affecting hepatocyte-dependent release of histidine-rich glycoprotein (HRGP)

To address the mechanisms by which hepatocyte HIF-2α up-regulation promotes inflammatory mechanisms in NAFLD we focused our attention on the role of histidine-rich glycoprotein (HRGP), a hepatocyte-released mediator (i.e., hepatokine) that has been recently shown to support liver macrophage activation in experimental and clinical NAFLD/NASH.[32] To investigate the possible hypoxia- and HIF-2α-dependent modulation of HRGP we employed HepG2 cells, which are known to rapidly respond to hypoxia with HIF-2α stabilization and the up-regulation of HIF-2α target genes.[28,33] As shown in Figure 5A the incubation of HepG2 cells under hypoxic condition, which is known to rapidly promote the nuclear translocation of HIF-2α,[28] was associated to an appreciable increase in HRGP synthesis. A very significant up-regulation of HRGP transcription was also observed in HepG2 transfected with an HIF-2α-containing, but not with an empty vector (Figure 5B), confirming a HIF-2α-dependent modulation of HRGP in liver cells. According with the in vitro data, hepatic HRGP transcript levels increased in a time-dependent manner in control mice fed with CDAA diet in parallel with the upregulation of the expression of another HIF-2α-dependent gene such as CXCR4 (Figure 5C). Conversely, HRGP up-regulation associated with NAFLD evolution was almost completely prevented at both mRNA and protein level in hHIF-2α$^{-/-}$ mice (Figure 5C,D). The relationships between HIF-2α and HRGP were further confirmed by the evidence that HepG2 stably transfected to overexpress HIF-2α also overexpressed transcript levels

of other HIF-2α target genes such as CXCR4 and erythropoietin (Suppl. Figure 5 A,B) or, as previously reported, SerpinB3. [28] Moreover, HRGP transcript and protein levels were down-regulated in HepG2 exposed to hypoxic conditions following efficient silencing for HIF-2α (Suppl. Figure 5 C,D). Immunohistochemistry performed on liver from mice fed with the CDAA diet confirmed that HRGP was selectively expressed by hepatocytes of control mice with steatohepatitis, but not in those from hHIF-2α$^{-/-}$ animals (Figure 5E). HIF-2α and HRPG up-regulation were unrelated to choline deficiency and were also observed in mice with NAFLD induced by administration in the drinking water of a high fat / fructose (HF/F) diet (Suppl. Figure 6 A-D). Hepatocyte-derived HRGP has been recently shown to promote liver inflammation by stimulating M1 polarization of hepatic macrophages.[32] In our hands, the impaired production of HRPG in mice receiving the CDAA diet decreased the liver infiltration by F4/80 positive macrophages as evidence by both immunohistochemistry (Figure 6A) and flow cytometry (Suppl. Fig 7A). Furthermore, the fraction of inflammatory Ly6C^{high} hepatic macrophages and their capacity to produce IL-12 was significantly lower in hHIF-2α$^{-/-}$ mice as compared to control littermates (Figure 6B). Consistently the hepatic expression of M1 cyto/chemokines TNFα, IL-12p40, CCL2 and CXCL10 (Suppl Figure 7B) and the serum levels of IL-12 were also significantly reduced in hHIF-2α$^{-/-}$ mice receiving the CDAA diet (Figure 6C) indicating a possible role of HRGP in the mechanisms by which the stimulation of HIF-2α in parenchymal cells supports pro-inflammatory responses of hepatic macrophages.

Finally, to further support the possible relevance of the relationships between HIF-2α and HRGP in the human disease, we analyzed for HIF-2α and HRGP immune-staining serial sections (4 μm thick) in our cohorts of NAFLD patients. Figure 7A shows that HRGP positivity was very low in sections from control livers. Conversely, in agreement with previous data,[32] HPRG immune-staining was well evident and increased in liver sample from NAFLD patients irrespectively from the disease

evolution (Figure 7B,C) and co-localized with that of HIF-2α (Figure 7A). Furthermore, we found a significant positive correlation between HIF-2α and HRGP mRNA levels in those patients of this cohort (n=19) for whom frozen liver specimens were available (Figure 7D).

Discussion

As mentioned in the introduction, hypoxia and HIFs have been proposed to play a role in the progression of CLD. [8-11] However, data concerning their role in the evolution of NAFLD are quite limited [10] and, more specifically, the contribution of HIF-2α has never been investigated in detail. In the present study we provide evidence that hepatocyte HIF-2α is up-regulated in either human or experimental NAFLD and we propose a mechanism by which HIF-2α activation in the liver parenchyma can contribute to the disease progression.

To our knowledge, the present study is the first to report that HIF-2α is specifically overexpressed in hepatocytes during the development of human NAFLD. In the majority of the liver biopsies from NAFLD patients a nuclear localization of HIF-2α is also evident, indicating that, by forming heterodimer with either HIF-1β or HIF-2β, HIF-2α can act as a transcription factor. Interestingly, HIF-2α activation is evident already in the early stage of the disease (F0-F1) and it is maintained up to more advanced (F3-F4) conditions of fibrosis/cirrhosis. Similar findings have been detected in murine models of NAFLD. In this setting, both HIF-2α and HIF-1α transcripts were up-regulated in mice with steatohepatitis, but only those of HIF-2α paralleled the disease progression. Altogether, these data suggest that HIF-dependent responses are an early event in NAFLD evolution and can be involved in the disease progression. Hepatic hypoxia likely represents the most obvious cause for HIF-2α up-regulation in both human and experimental NAFLD. In fact,

diffuse lobular staining with the hypoxia-sensitive dye pimonidazole has recently documented in mice with NAFLD. [21] Nevertheless, we cannot exclude that hypoxia-independent mechanisms, as for instance oxidative stress, might also contribute to stimulate HIF-2α activity. [8-11]

The actual relevance of HIF-2α in NAFLD progression has been mechanistically confirmed by inducing NAFLD with MCD or CDAA diets in mice carrying a hepatocyte specific deletion of HIF-2α (hHIF-2α$^{-/-}$ mice). We have observed that steatosis, parenchymal injury, inflammatory response and liver fibrosis are appreciably attenuated in these animals, as compared with control littermates. The decrease in fatty liver detected in hHIF-2α$^{-/-}$ mice is consistent with the observation that HIF-2α activation is *per se* capable to promote fatty liver by up-regulating genes involved in fatty acid synthesis/uptake and lipid storage and by down-regulating those involved in fatty acid catabolism. [18,19] Accordingly, in the CDAA diet model transcript levels of SREBP1 and of FASN (Fatty Acid Synthase) were significantly reduced in hHIF-2α-/- mice vs related control littermates exposed to the same diet (Suppl. Figure 8). Moreover, by employing murine hepatocytes (AML12 line), we found that exposure of these cells to palmitic acid (i.e, a condition leading to lipid accumulation and mimicking “in vitro” lipotoxicity) resulted in a significant up-regulation of both HIF-2α and HRGP protein levels (Suppl. Figure 9A) and of HRGP transcript levels (Suppl. Figure 9B), suggesting that also lipotoxicity may represent an additional condition leading to HIF-2α and HRGP up-regulation.

Furthermore, in a previous study using mice fed with a high fat diet the hepatocyte deletion of HIF-1α effectively prevented NAFLD associated liver fibrosis without interfering with fat accumulation. [21] Interestingly, the same work also showed that hepatocyte HIF-1α deficiency moderately affected parenchymal damage and did not influenced the extent of lobular inflammation. [21] This indicates that beside the action on steatosis, the activation of HIF-2α in hepatocytes has a key role in favoring NAFLD-associated cell injury and inflammatory responses.

To investigate whether hepatocyte HIF-2α might stimulate the production of mediators with pro-inflammatory action, we focused the attention on the possible role of HRGP, a multifunctional hepatocyte-derived circulating protein, [34] that has been recently shown to be involved in modulating pro-inflammatory activity of macrophages in tumors as well during chronic liver injury. [32,35] In particular, Bartneck et al. [32] have reported that HRGP deletion leads to a significant protection from liver injury and fibrosis in mice with MCD-induced NASH by down-modulating the recruitment of hepatic macrophages, and their M1 polarization. In this setting, our data demonstrate an interplay between HIF-2α and HRGP during NAFLD evolution by showing that the lack of hepatocyte HIF-2α prevents HRGP up-regulation in mice fed with CDAA diet. Furthermore, HRGP staining of liver biopsies from NAFLD patients co-localizes with that of HIF-2α, while in the same subjects a positive linear correlation is evident between the HIF-2α and HRGP transcripts. These findings are supported by in vitro experiments employing HepG2 cells exposed to hypoxia or overexpressing HIF-2α that confirm the strict HIF-2α dependence of HRGP production.

In line with the view that HIF-2α deficiency can reduce hepatic inflammation by preventing HRGP-mediated support to M1 activation of liver macrophages, we have observed that the liver expression of M1 markers TNF-α, IL-12and CXCL10 is blunted in hHIF-2α$^{-/-}$ mice with NAFLD. Moreover, flow cytometry reveals that the prevalence of pro-inflammatory Ly6C^{high} hepatic macrophages and their capacity to produce IL-12 are lowered in hHIF-2α$^{-/-}$ mice fed the CDAA diet. HIF-2α influence on macrophage responses is of potential general relevance since it is well known that the polarization of hepatic macrophages is a crucial determinant for the progression of CLDs. [36] In particular, macrophage M1 shift has been reported to correlate with the severity of both alcoholic and non-alcoholic liver disease. [37,38] Accordingly, M2 skewing is associated with a more favorable histology and fewer hepatic lesions in patients with ethanol-related CLD [37] as well as in HRGP$^{-/-}$ mice exposed to chronic liver injury. [32]

The involvement of HRGP in mediating the effects of HIF-2α activation during NAFLD progression does not rule out the possible involvement of other mediators. We have previously reported that HIF-2α activation in human liver cancer cells up-regulates Serpin B3 and this latter contributes to the development of fibrosis during CLD by sustaining the most relevant profibrogenic responses by activated stellated cells.[28,30] Unfortunately, at difference of humans, SerpinB3 is virtually undetectable in murine livers during CLD, thus in the present study we did not have the possibility to evaluate its contribution to NAFLD progression. However, based on the association between circulating levels of Serpin B3 and the risk of fibrosis in patients with chronic hepatitis C,[39] a possible role of Serpin B3 in the evolution of human NAFLD cannot be excluded.

In conclusion, data presented indicate that hepatocyte HIF-2α activation during the evolution of human and murine NAFLD has a role in the disease progression by mediating the up-regulation of HRGP expression that, in turn critically influence the severity of steatohepatitis and fibrogenesis. These findings point HIF-2α and HIF-2α-dependent genes as putative targets for future therapeutic strategies in NAFLD, a disease that, at present, has no validated therapy.

REFERENCES

1) Satapathy SK, Sanyal AJ. Epidemiology and Natural History of Nonalcoholic Fatty Liver Disease. Semin Liver Dis 2015;35:221-235.

2. Younossi ZM, Koenig AB, Abdelatif D, Fazel Y, Henry L, Wymer M. Global epidemiology of non-alcoholic fatty liver disease - Meta-analytic assessment of prevalence, incidence and outcomes. Hepatology 2016;64:73-84.

3. Yki-Jarvinen H. Non-alcoholic fatty liver disease as a cause and a consequence of metabolic syndrome. Lancet Diabetes Endocrinol 2014;2:901-910

4. McPherson S, Hardy T, Henderson E, Burt AD, Day CP, Anstee QM. Evidence of NAFLD progression from steatosis to fibrosing-steatohepatitis using paired biopsies: Implications for prognosis and clinical management. J Hepatol 2015;62:1148-1155.

5. Singh S, Allen AM, Wang Z, Prokop LJ, Murad MH, Loomba R. Fibrosis progression in nonalcoholic fatty liver vs nonalcoholic steatohepatitis: a systematic review and meta-analysis of paired-biopsy studies. Clin Gastroenterol Hepatol 2015;13:643–54.e9.

6. Adams LA, Anstee QM, Tilg H, Targher G. Non-alcoholic fatty liver disease and its relationship with cardiovascular disease and other extrahepatic diseases. Gut 2017;66:1138-1153.

7. Torres DM, Harrison SA. Nonalcoholic steatohepatitis and noncirrhotic hepatocellular carcinoma: fertile soil. Semin Liver Dis 2012;32:30-8.

8. Nath B, Szabo G. Hypoxia and hypoxia inducible factors: diverse roles in liver diseases. Hepatology 2012;55:622-633.

9. Wilson GK, Tennant DA, McKeating JA. Hypoxia inducible factors in liver disease and hepatocellular carcinoma: current understanding and future directions. J Hepatol. 2014 ;61:1397-1406.

10. Lefere S, Van Steenkiste C, Verhelst X, Van Vlierberghe H, Devisscher L, Geerts A. Hypoxia - regulated mechanisms in the pathogenesis of obesity and non-alcoholic fatty liver disease. Cell. Mol Life Sci 2016; 73:3419-3431.

11. Novo E, Cannito S, Paternostro C, Bocca C, Miglietta A, Parola M. Cellular and molecular mechanisms in liver fibrogenesis. Arch Biochem Biophys 2014;548:20-37.

12. Semenza GL. Oxygen sensing, hypoxia-inducible factors, and disease pathophysiology. Annu Rev Pathol 2014;9:47–71.

13. Shay JE, Simon MC. Hypoxia-inducible factors: crosstalk between inflammation and metabolism. Semin Cell Dev Biol 2012;23:389-394.

14. **Majmundar AJ**, **Wong WJ**, Simon MC. Hypoxia-inducible factors and the response to hypoxic stress. Mol Cell 2010;40:294-309.

15. Arteel GE, Iimuro Y, Yin M, Raleigh JA, Thurman RG. Chronic enteral ethanol treatment causes hypoxia in rat liver tissue in vivo. Hepatology 1997;25:920–926.

16. Mantena SK, Vaughn DP, Andringa KK, Eccleston HB, King AL, Abrams GA, et al. High fat diet induces dysregulation of hepatic oxygen gradients and mitochondrial function in vivo. Biochem J 2009;417:183–193.

17. Nakazawa MS, Keith B, Simon MC. Oxygen availability and metabolic adaptations. Nat Rev Cancer 2016;16:663-73.

18. Rankin EB, Rha J, Selak MA, Unger TL, Keith B, Liu Q et al. Hypoxia-inducible factor 2 regulates hepatic lipid metabolism. Mol Cell Biol 2009;29:4527-4538.

19. Qu A, Taylor M, Xue X, Matsubara T, Metzger D, Chambon P, et al. Hypoxia-inducible transcription factor 2α promotes steatohepatitis through augmenting lipid accumulation, inflammation, and fibrosis. Hepatology 2011;54:472-483.

20. Moon JO, Welch TP, Gonzalez FJ, Copple BL. Reduced liver fibrosis in hypoxia-inducible factor-1a-deficient mice. Am J Physiol Gastrointest Liver Physiol 2009; 296:G582–G592.

21. Nath B, Levin I, Csak T, Petrasek J, Mueller C, Kodys K, et al. Hepatocyte-specific hypoxia-inducible factor-1α is a determinant of lipid accumulation and liver injury in alcohol-induced steatosis in mice. Hepatology 2011;53:1526-1537.

22. Mesarwi OA, Shin MK, Bevans-Fonti S, Schlesinger C, Shaw J, Polotsky VY. Hepatocyte Hypoxia Inducible Factor-1 Mediates the Development of Liver Fibrosis in a Mouse Model of Nonalcoholic Fatty Liver Disease. PLoS One. 2016;11:e0168572.

23. Nishiyama Y, Goda N, Kanai M, Niwa D, Osanai K, Yamamoto Y, et al. HIF-1α induction suppresses excessive lipid accumulation in alcoholic fatty liver in mice. J Hepatol 2012; 56:441–447.

24. Ochiai D, Goda N, Hishiki T, Kanai M, Senoo-Matsuda N, Soga T, et al. Disruption of HIF-1α in hepatocytes impairs glucose metabolism in diet-induced obesity mice. Biochem Biophys Res Commun 2011;415:445–449.

25. Kleiner DE, Brunt EM, Van Natta M, Behling C, Contos MJ, Cummings OW, et al. Design and validation of a histological scoring system for nonalcoholic fatty liver disease. Hepatology 2005;41:1313-1321.

26. Locatelli I, Sutti S, Jindal A, Vacchiano M, Bozzola C, Reutelingsperger C, et al. Endogenous annexin A1 is a novel protective determinant in nonalcoholic steatohepatitis in mice. Hepatology 2015; 60:531-544.

27. De Minicis S, Agostinelli L, Rychlicki C, Sorice GP, Saccomanno S, Candelaresi C, et al. HCC development is associated to peripheral insulin resistance in a mouse model of NASH. Plos One 2014; 9(5):e97136.

28. **Cannito S**, **Turato C**, Paternostro C, Biasiolo A, Colombatto S, Cambieri I, et al. Hypoxia up-regulates SERPINB3 through HIF-2α in human liver cancer cells. Oncotarget 2015; 6:2206-2221.

29. **Novo E**, **Busletta C**, Valfrè di Bonzo L, Povero D, Paternostro C, Mareschi K, et al. Intracellular reactive oxygen species are required for directional migration of resident and bone marrow-derived hepatic pro-fibrogenic cells. J Hepatol 2011;54:964-974.

30. **Novo E**, **Villano G**, Turato C, Cannito S, Paternostro C, Busletta C, et al. SerpinB3 promotes pro-fibrogenic responses in activated hepatic stellate cells. Scientific Reports 2017;7(1):3420.

31. Sutti S, Jindal A, Locatelli I, Vacchiano M, Gigliotti L, Bozzola C, et al. Adaptive immune responses triggered by oxidative stress contribute to hepatic inflammation in NASH. Hepatology 2014;59:886-897.

32. **Bartneck M**, **Fech V**, Ehling J, Govaere O, Warzecha KT, Hittatiya K, et al. Histidine-rich glycoprotein promotes macrophage activation and inflammation in chronic liver disease. Hepatology 2016;63:1310-1324.

33. **Turato C**, **Cannito S**, Simonato D, Villano G, Morello E, Terrin L, et al. SerpinB3 and Yap Interplay Increases Myc Oncogenic Activity. Sci Rep 2016; 5:17701.

34. Hulett MD, Parish CR. Murine histidine-rich glycoprotein: cloning, characterization and cellular origin. Immunol Cell Biol 2000;78:280-287.

35. **Rolny C**, **Mazzone M**, Tugues S, Laoui D, Johansson I, Coulon C, et al. HRG inhibits tumor growth and metastasis by inducing macrophage polarization and vessel normalization through downregulation of PlGF. Cancer Cell 2011;19:31-44.

36. Tacke F, Zimmermann HW. Macrophage heterogeneity in liver injury and fibrosis. J Hepatol 2014;60:1090-1096.

37. **Wan J**, **Benkdane M**, Teixeira-Clerc F, Bonnafous S, Louvet A, Lafdil F, et al. M2 Kupffer cells promote M1 Kupffer cell apoptosis: a protective mechanism against alcoholic and nonalcoholic fatty liver disease. Hepatology 2014;59:130-142.

38. Wan J, Benkdane M, Alons E, Lotersztajn S, Pavoine C. M2 kupffer cells promote hepatocyte senescence: an IL-6-dependent protective mechanism against alcoholic liver disease. Am J Pathol 2014;184:1763-1772.

39. Biasiolo A, Chemello L, Quarta S, Cavalletto L, Bortolotti F, Caberlotto C, et al. Monitoring SCCA-IgM complexes in serum predicts liver disease progression in patients with chronic hepatitis. J Viral Hep 2008;15: 246-249.

Author names in bold designate shared co-first authorship.

Figure Legends

Figure 1. **Expression of HIF-2α in human liver disease.** Immunohistochemistry analysis of HIF-2α in paraffin-embedded human liver specimens from NAFLD patients (n = 27) with different degrees of liver fibrosis (F0-F4) (**A**). Control liver refer to surgical resections for hepatic metastasis of colon carcinoma (magnification 20X, 40X, 100X). HIF-2α expression was semi-quantitatively scored blinded, by a pathologist. $P < 0.05$ (Mann-Whitney's U test). (**B**).

Figure 2. Liver injury and inflammatory markers in hHIF2α $^{-/-}$ and control mice with NAFLD induced by feeding a MCD diet. hHIF2α$^{-/-}$ and wild type littermates (LM) were fed a MCD diet for 4 weeks and the following parameters were evaluated: **(A-C)** Parenchymal injury and liver steatosis, as evaluated by measuring **(A)** serum levels of alanine (ALT)**, (B)** hepatic TG content **or,** morphologically, by hematoxylin/eosin staining (magnification 10X) **(C)**; **(D)** Liver expression of inflammatory markers TNF-α, CD11b and CCL2, as evaluated by quantitative real-time PCR (Q-PCR). The mRNA values are expressed as fold increase over control values after normalization to the β-actin gene expression and are means ± SD of 6-8 animals per group. The boxes include the values within 25th and 75th percentile, while the horizontal bars represent the medians. The extremities of the vertical bars (10th-90th percentile) comprise the eighty percent of the values. Statistical differences were assessed by one-way ANOVA test with Tukey's correction for multiple comparisons.

Figure 3. **Liver injury in hHIF2α$^{-/-}$ and control mice fed with a CDAA diet**. hHIF2α$^{-/-}$ and wild type littermates (LM) were fed CDAA diet for 12 or 24 weeks and the following parameters were evaluated: Parenchymal injury, as evaluated by measuring the serum levels of alanine (ALT) **(A)** or hepatic TG content **(B);** Body weight change **(C)** and plasma glucose concentration (**D**). Liver morphology in mice exposed to CDAA diet was evaluated by hematoxylin/eosin staining

(magnification 10X) (**E**). The values are means ± SD and refer to 6-8 animals per group. Statistical differences were assessed by one-way ANOVA test with Tukey's correction for multiple comparisons.

Figure 4. **Liver fibrosis "in vivo" in hHIF-2α$^{-/-}$ mice vs LM mice fed with CDAA diet**. Liver fibrosis was evaluated morphologically in hHIF-2α$^{-/-}$ mice and wild type littermates (LM) mice following 12 or 24 weeks on the CDAA or control CSAA diets by Sirius red staining (**A**) and immunohistochemistry for α-SMA (**D**). Original magnification as indicated. ImageJ software analysis was performed for Sirius red staining to evaluate the amount of fibrosis **(B)**. Analysis by quantitative real-time PCR (Q-PCR) of transcript levels of pro-fibrogenic genes collagen 1A1, αSMA, TGFβ1 in the different experimental groups (**C**). The values are means ± SD and refer to 6-8 animals per group. Statistical differences were assessed by one-way ANOVA test with Tukey's correction for multiple comparisons.

Figure 5. Modulatory effect of HIF2α on HRGP. Western blotting analysis of HIF2α and HRGP levels in HepG2 cells exposed to hypoxic conditions (**A**). Q-PCR analysis of HRGP transcript in control HepG2 cells (HepG2 C: not transfected; EV: transfected with empty vector) or HepG2 cells stably transfected to over-express HIF-2α (**B**). Data in graphs are expressed as means ± SEM. qPCR analysis of HRGP and CXCR4 transcripts in wild type littermates (LM) or hHIF-2α$^{-/-}$ mice fed with the control diet (CSAA) or with the CDAA diet for 12 and 24 weeks (**C**). Hepatic mRNAs was as fold increase over control values after normalization to the β-actin gene expression. The values are means ± SD and refer to 6-8 animals per group. Statistical differences were assessed by one-way ANOVA test with Tukey's correction for multiple comparisons). Western blotting analysis of HRGP levels in liver of hHIF-2α$^{-/-}$ and littermate mice fed with CDAA diet for 24 weeks (**D**). Histograms report densitometric analyses normalized for the relative GAPDH content. Localization of HRGP expression by IHC in the livers of wild type littermates (LM) or hHIF-2α$^{-/-}$ CDAA or CSAA fed

animals. Original magnification as indicated. ImageJ software analysis was performed for quantification of HRGP staining (**E**). Data are expressed as means ± SD.

Figure 6. Inflammatory markers in hHIF-2α$^{-/-}$ and control mice fed with a CDAA diet. hHIF-2α$^{-/-}$ and wild type littermates (LM) mice were fed with a CDAA diet or CSAA diet for 12 or 24 weeks and the detection of macrophages positive for F4/80 was evaluated by IHC (original magnification as indicated). ImageJ software analysis was performed for quantification of F4/80 staining (**A**). Data are expressed as means ± SD. Hepatic myeloid cells were isolated from livers of either hHIF-2α$^{-/-}$ mice and wild type littermates (LM) fed with the CDAA diet analyzed by flow cytometry for Ly6C and IL expression in Cd11b/F4-80-positive liver macrophages. (**B**) Data are expressed as means ± SD. Circulating IL-12 levels were determined by ELISA assay (**C**). Values refer to 6-8-10 animals per group; boxes include the values within 25th and 75th percentile, whereas horizontal bars represent the medians. The extremities of the vertical bars (10th-90th percentile) comprise 80% of the values. Statistical differences were assessed by one-way ANOVA test with Tukey's correction for multiple comparisons.

Figure 7. HRGP expression in human livers with NASH. HRGP detection by IHC in liver specimens from NASH patients (n =27) with different degrees of liver fibrosis (F0-F4, NAS 2-6). Control liver sample refer to surgical resections for hepatic metastasis of colon carcinoma. Original magnification as indicated. ImageJ software analysis was performed for quantification of HRGP staining (**A**). Data are expressed as means ± SD. HRGP expression was semi-quantitatively scored by a pathologist. P value were calculated with Mann-Whitney's U test (**B**). Relationship between HRGP and HIF2α mRNA in human NASH patients (F0-F4, NAS 2-6) (**C**). The values represent the relative mRNA content. The correlation analysis was performed with Spearman r test.

Figure 1

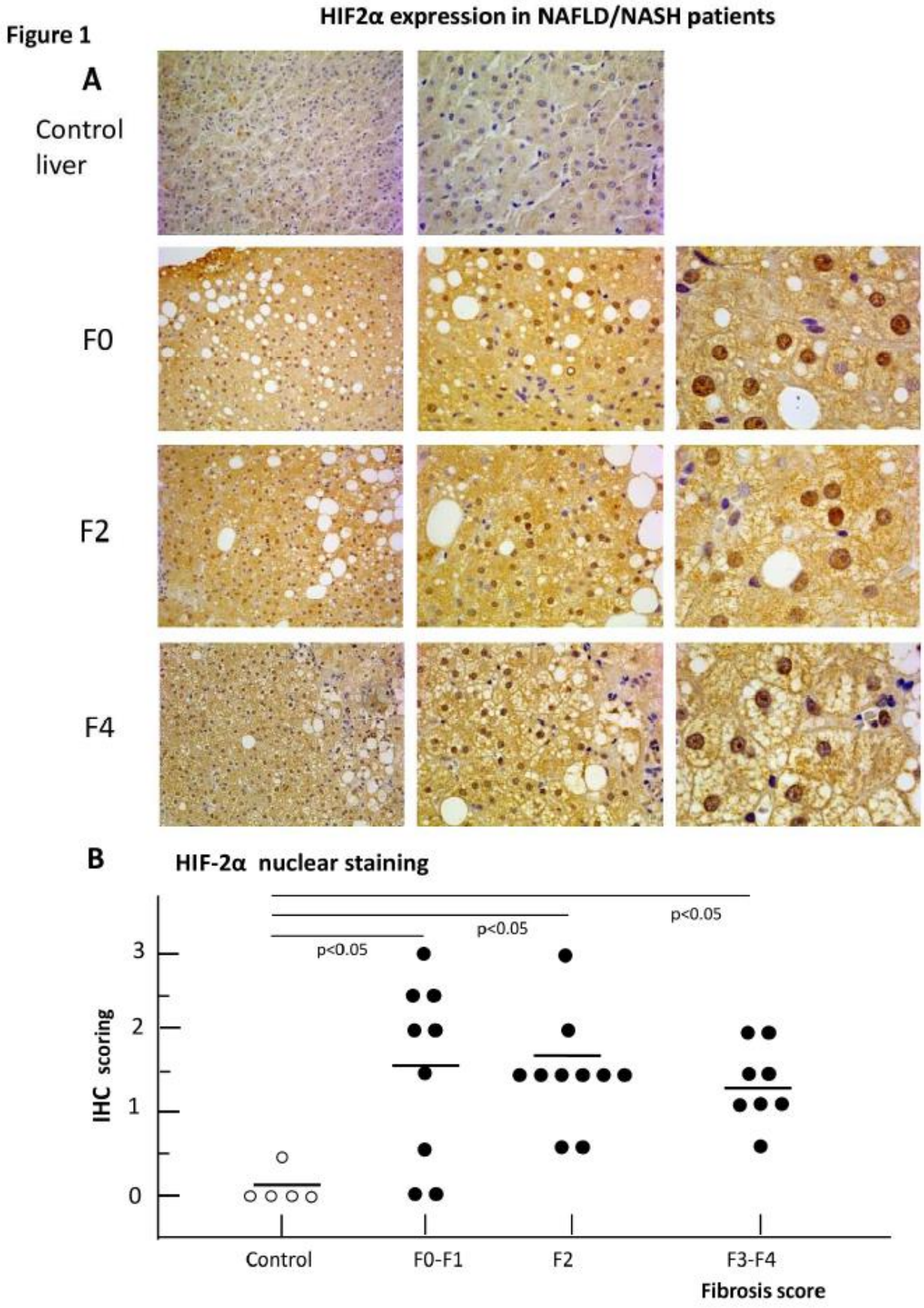
HIF2α expression in NAFLD/NASH patients
A
Control liver
F0
F2
F4
B
HIF-2α nuclear staining
p<0.05
p<0.05
p<0.05
IHC scoring
0
1
2
3
Control
F0-F1
F2
F3-F4
Fibrosis score

Figure 2

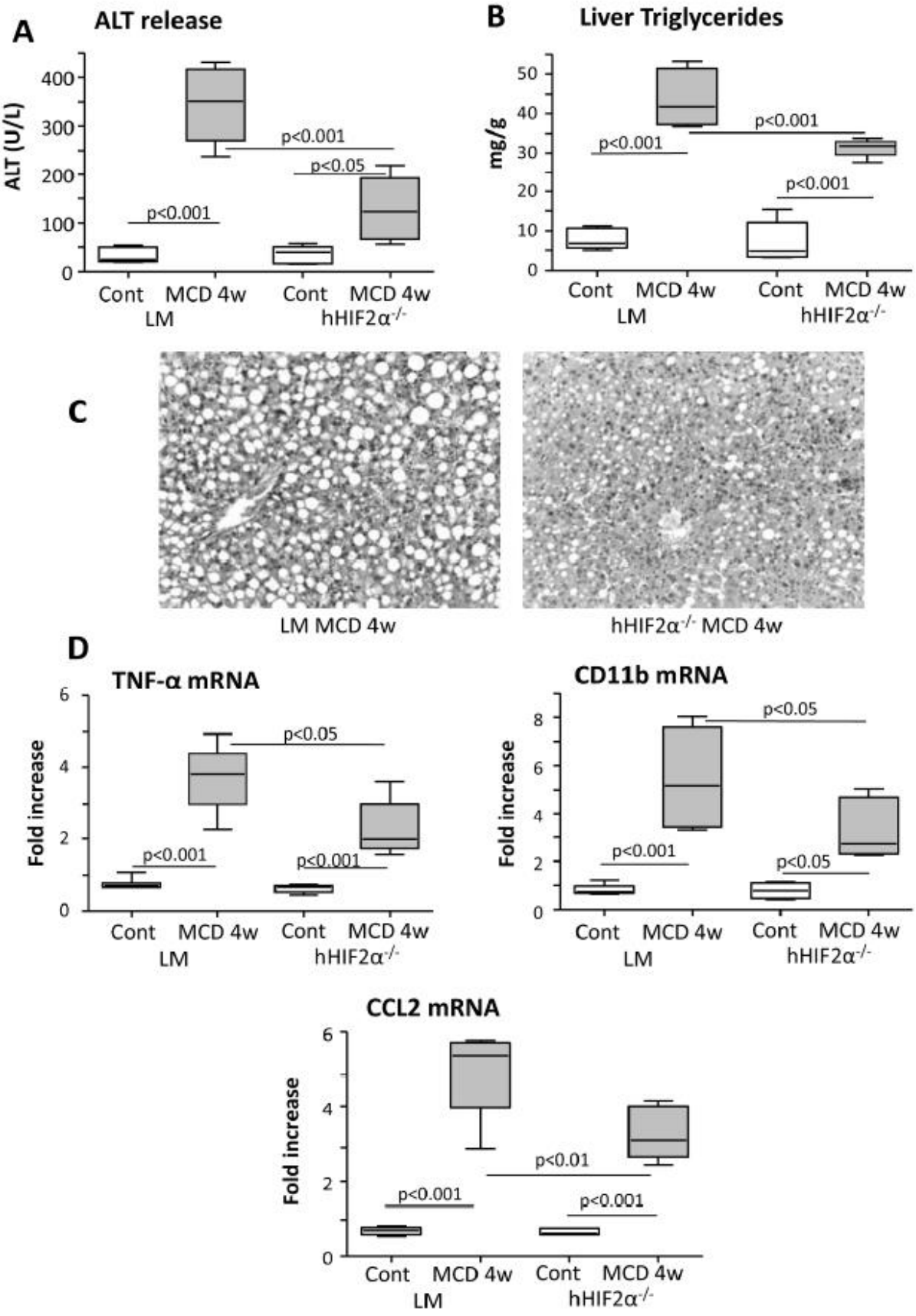
A
ALT release
ALT (U/L)
400
300
200
100
0
p<0.001
p<0.001
p<0.05
Cont
MCD 4w
Cont
MCD 4w
LM
hHIF2α-/-
B
Liver Triglycerides
mg/g
50
40
30
20
10
0
p<0.001
p<0.001
p<0.001
Cont
MCD 4w
Cont
MCD 4w
LM
hHIF2α-/-
C
LM MCD 4w
hHIF2α-/- MCD 4w
D
TNF-α mRNA
Fold increase
6
4
2
0
p<0.001
p<0.05
p<0.001
Cont
MCD 4w
Cont
MCD 4w
LM
hHIF2α-/-
CD11b mRNA
Fold increase
8
6
4
2
0
p<0.001
p<0.05
p<0.05
Cont
MCD 4w
Cont
MCD 4w
LM
hHIF2α-/-
CCL2 mRNA
Fold increase
6
4
2
0
p<0.001
p<0.01
p<0.001
Cont
MCD 4w
Cont
MCD 4w
LM
hHIF2α-/-

Figure 3

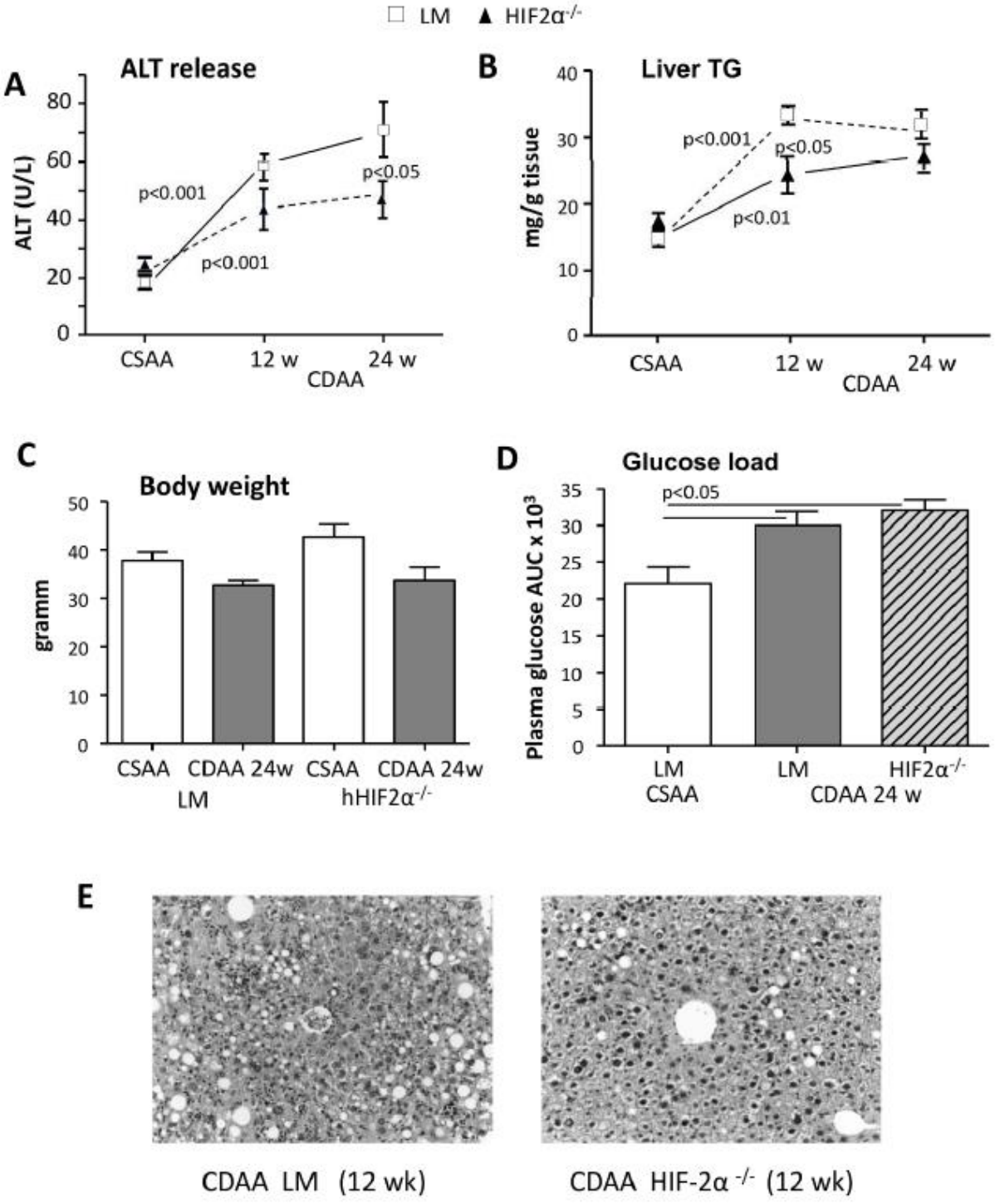
LM
HIF2α-/-
A
ALT release
ALT (U/L)
p<0.001
p<0.001
p<0.05
CSAA
12 w
24 w
CDAA
B
Liver TG
mg/g tissue
p<0.001
p<0.05
p<0.01
CSAA
12 w
24 w
CDAA
C
Body weight
gramm
CSAA
CDAA 24w
CSAA
CDAA 24w
LM
hHIF2α-/-
D
Glucose load
Plasma glucose AUC x 10³
p<0.05
LM
CSAA
LM
HIF2α-/-
CDAA 24 w
E
CDAA LM (12 wk)
CDAA HIF-2α -/- (12 wk)

Figure 4

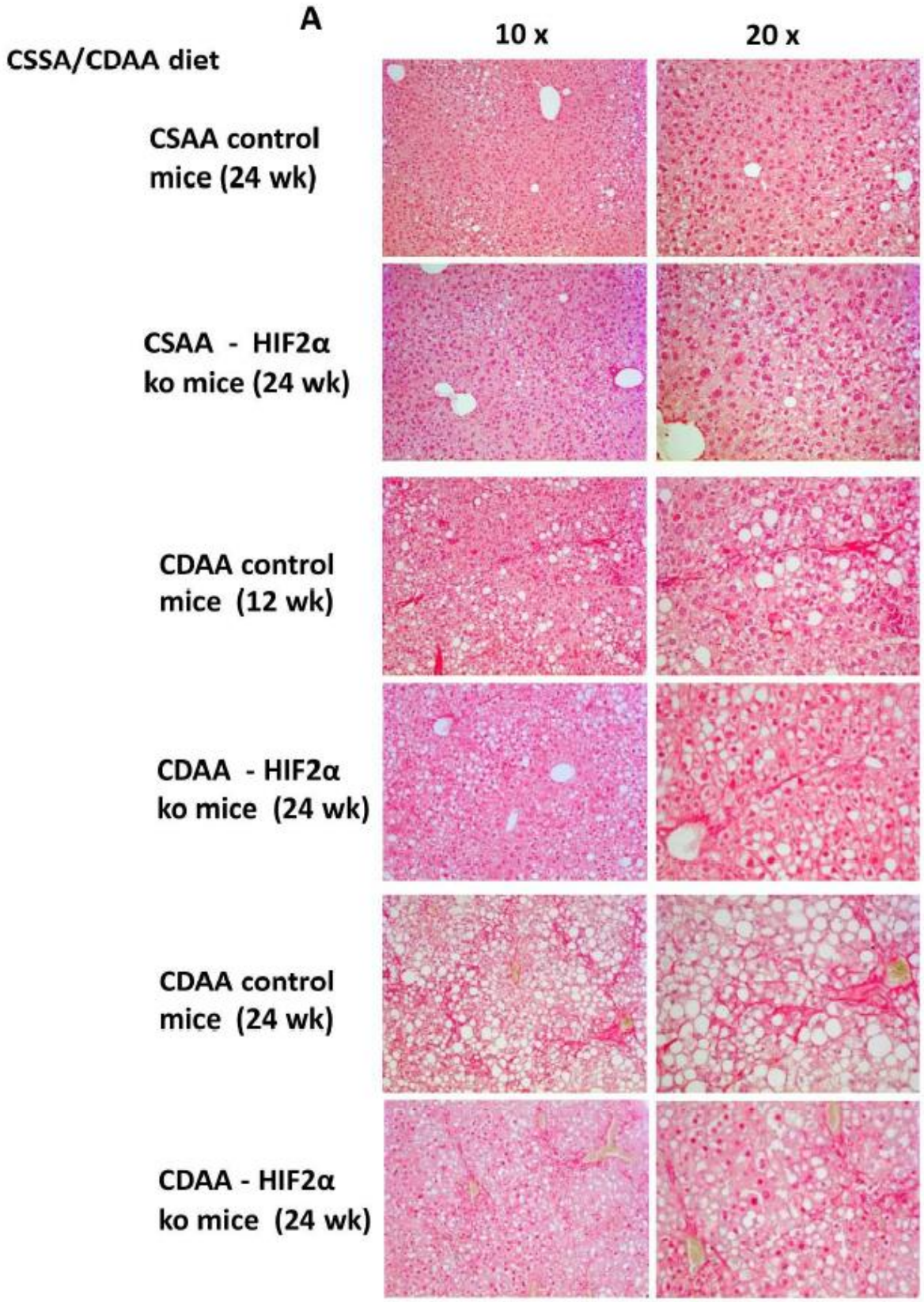
A
CSSA/CDAA diet
10 x
20 x
CSAA control mice (24 wk)
CSAA - HIF2α ko mice (24 wk)
CDAA control mice (12 wk)
CDAA - HIF2α ko mice (24 wk)
CDAA control mice (24 wk)
CDAA - HIF2α ko mice (24 wk)

Figure 4

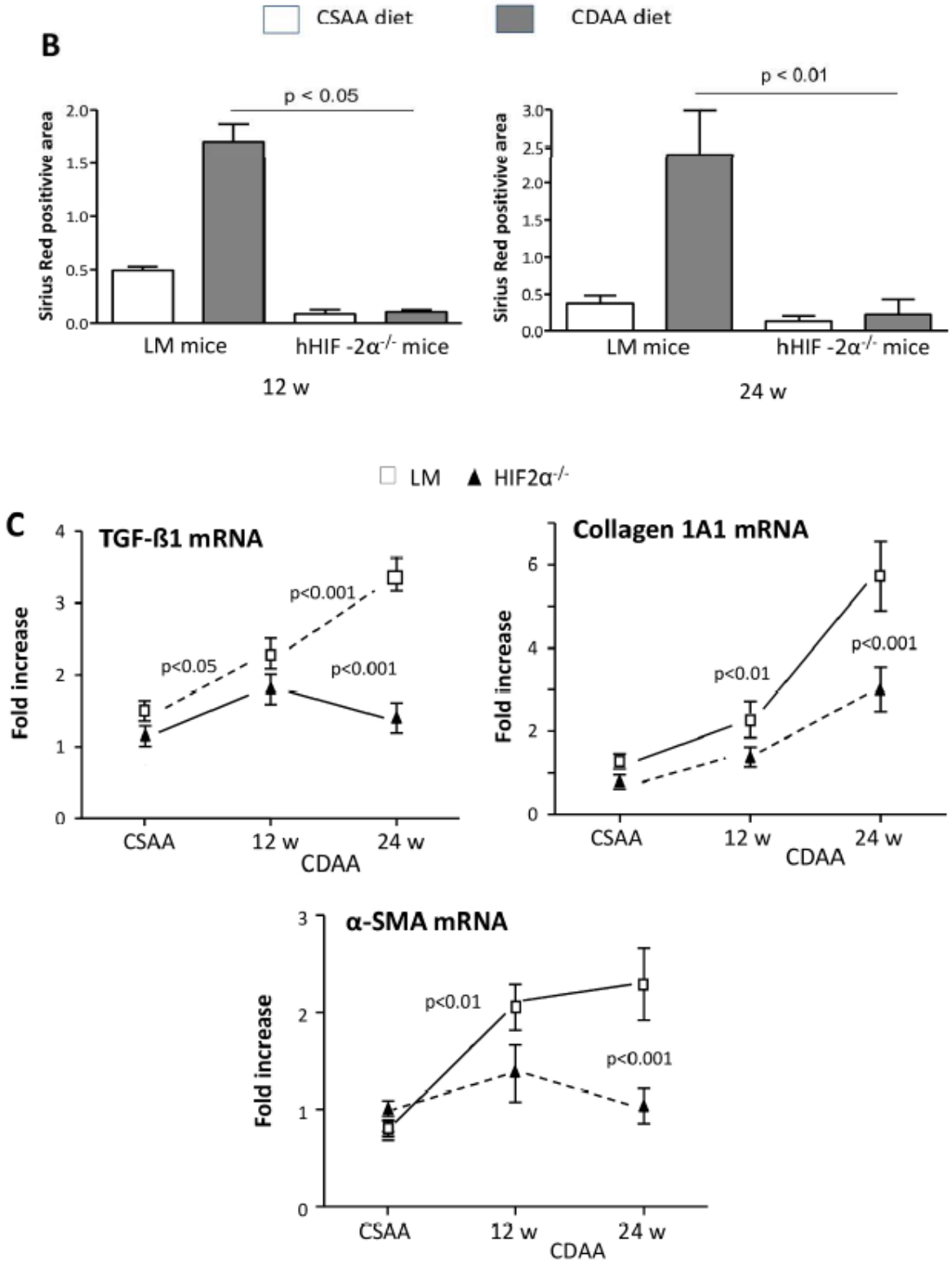
CSAA diet
CDAA diet
B
p < 0.05
Sirius Red positivive area
LM mice
hHIF -2α-/- mice
12 w
p < 0.01
Sirius Red positivive area
LM mice
hHIF -2α-/- mice
24 w
LM
HIF2α-/-
C
TGF-ß1 mRNA
Fold increase
p<0.05
p<0.001
p<0.001
CSAA
12 w
24 w
CDAA
Collagen 1A1 mRNA
Fold increase
p<0.01
p<0.001
CSAA
12 w
24 w
CDAA
α-SMA mRNA
Fold increase
p<0.01
p<0.001
CSAA
12 w
24 w
CDAA

Figure 4

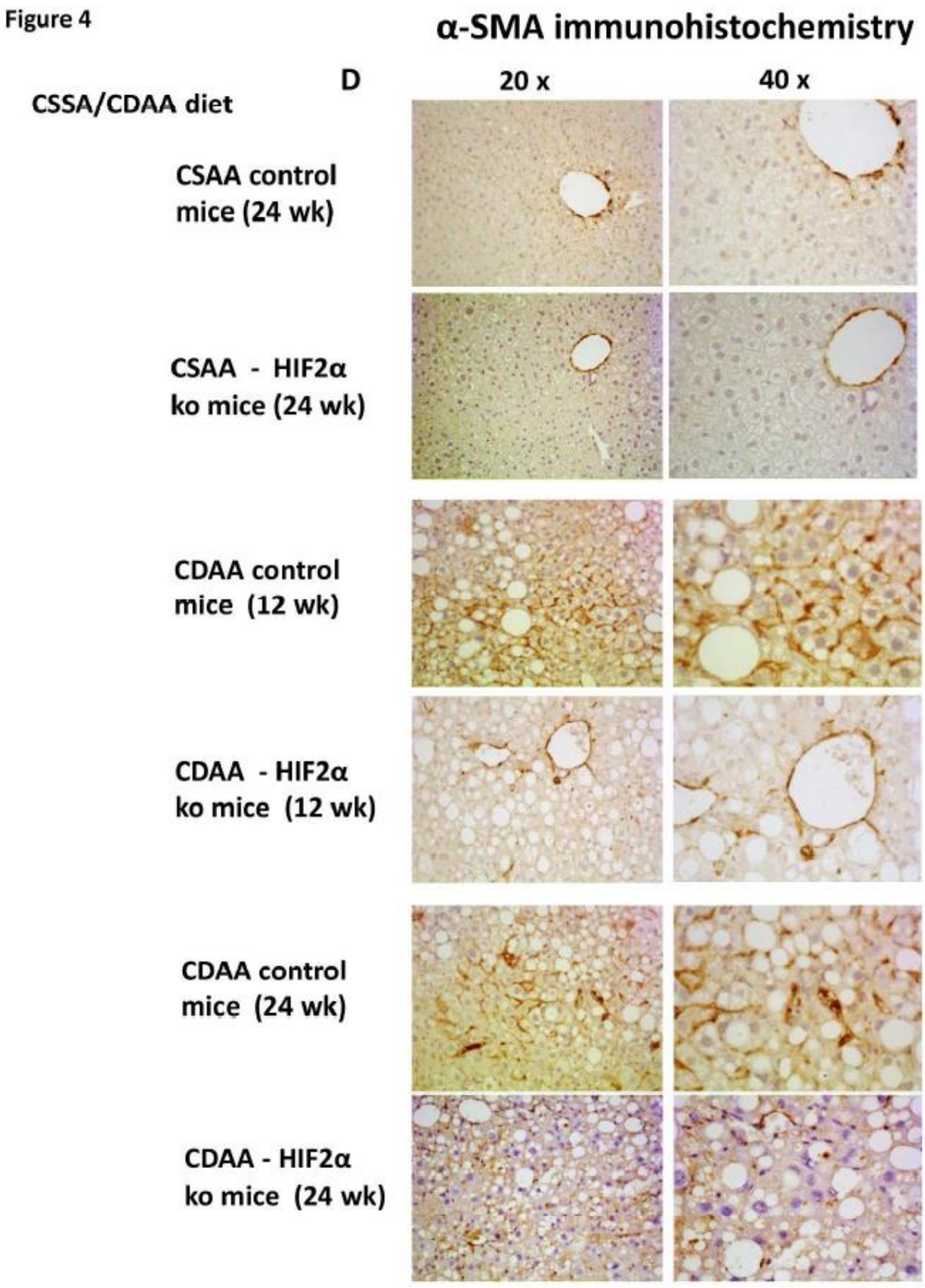
α-SMA immunohistochemistry
D
20 x
40 x
CSSA/CDAA diet
CSAA control mice (24 wk)
CSAA - HIF2α ko mice (24 wk)
CDAA control mice (12 wk)
CDAA - HIF2α ko mice (12 wk)
CDAA control mice (24 wk)
CDAA - HIF2α ko mice (24 wk)

Figure 5

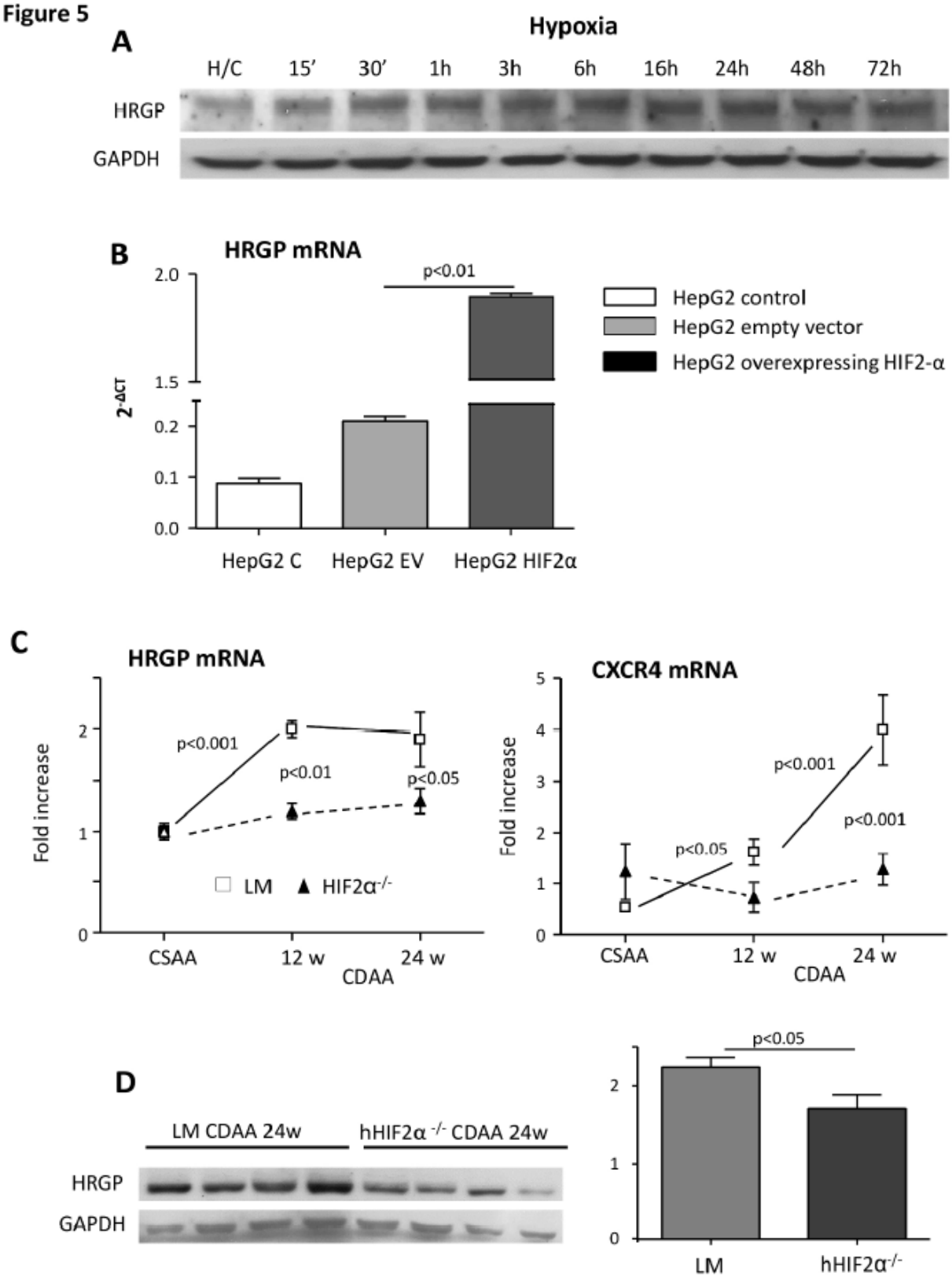
A
Hypoxia
H/C
15'
30'
1h
3h
6h
16h
24h
48h
72h
HRGP
GAPDH
B
HRGP mRNA
p<0.01
2.0
1.5
0.2
0.1
0.0
2-ΔCT
HepG2 C
HepG2 EV
HepG2 HIF2α
HepG2 control
HepG2 empty vector
HepG2 overexpressing HIF2-α
C
HRGP mRNA
p<0.001
p<0.01
p<0.05
Fold increase
LM
HIF2α-/-
CSAA
12 w
24 w
CDAA
CXCR4 mRNA
p<0.001
p<0.05
p<0.001
Fold increase
CSAA
12 w
24 w
CDAA
D
LM CDAA 24w
hHIF2α -/- CDAA 24w
HRGP
GAPDH
p<0.05
LM
hHIF2α-/-

Figure 5

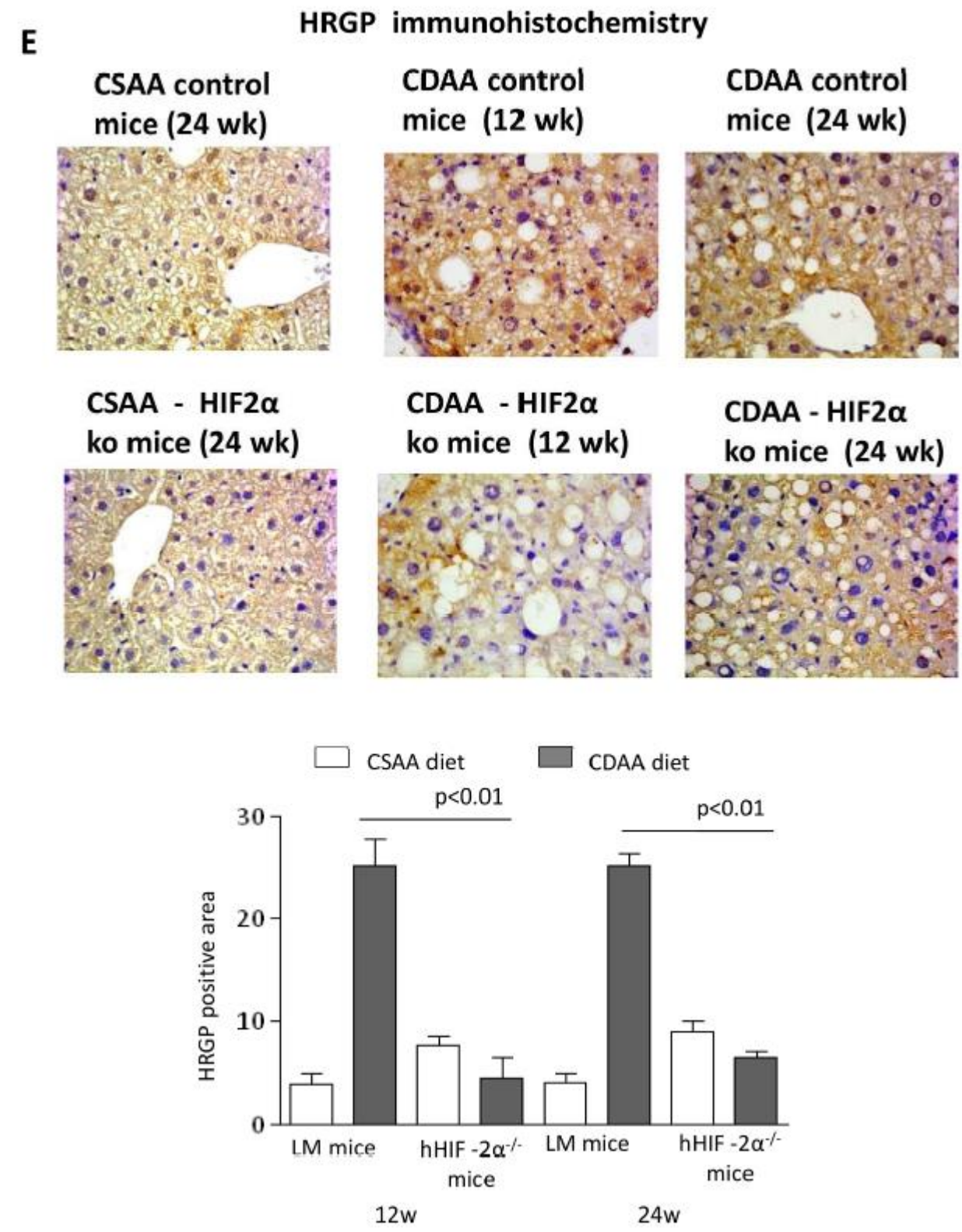
E
HRGP immunohistochemistry
CSAA control mice (24 wk)
CDAA control mice (12 wk)
CDAA control mice (24 wk)
CSAA - HIF2α ko mice (24 wk)
CDAA - HIF2α ko mice (12 wk)
CDAA - HIF2α ko mice (24 wk)
CSAA diet
CDAA diet
p<0.01
p<0.01
HRGP positive area
30
20
10
0
LM mice
hHIF -2α-/- mice
LM mice
hHIF -2α-/- mice
12w
24w

Figure 6

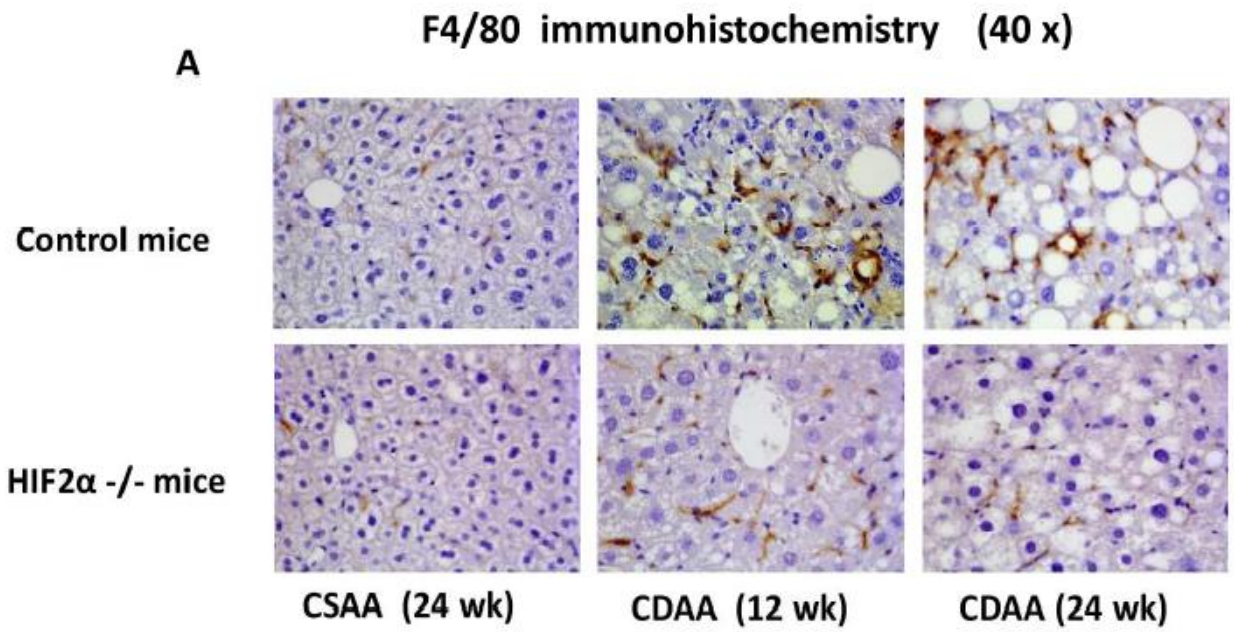
A
F4/80 immunohistochemistry (40 x)
Control mice
HIF2α -/- mice
CSAA (24 wk)
CDAA (12 wk)
CDAA (24 wk)

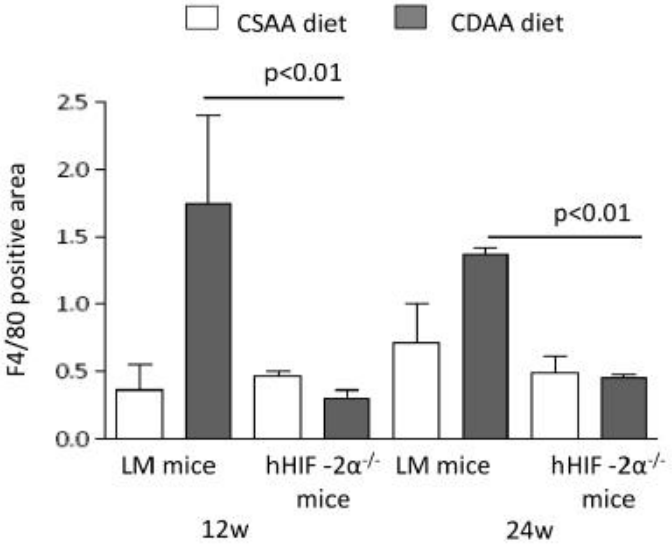
CSAA diet
CDAA diet
p<0.01
p<0.01
F4/80 positive area
2.5
2.0
1.5
1.0
0.5
0.0
LM mice
hHIF -2α-/- mice
LM mice
hHIF -2α-/- mice
12w
24w

Figure 6

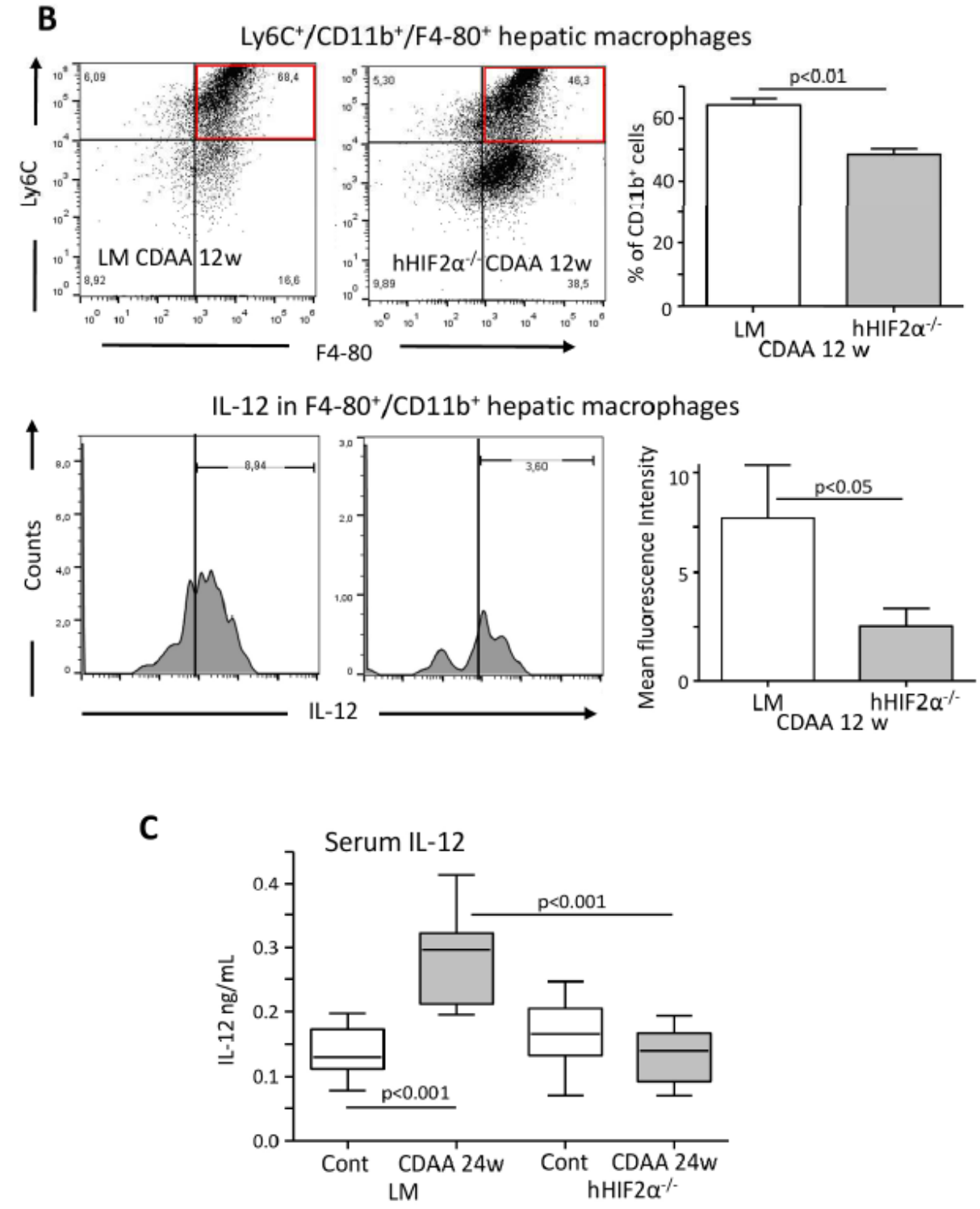
B
Ly6C+/CD11b+/F4-80+ hepatic macrophages
Ly6C
F4-80
6,09
68,4
8,92
16,6
LM CDAA 12w
5,30
46,3
9,89
38,5
hHIF2α-/- CDAA 12w
p<0.01
% of CD11b+ cells
LM
hHIF2α-/-
CDAA 12 w
IL-12 in F4-80+/CD11b+ hepatic macrophages
Counts
IL-12
8,94
3,60
p<0.05
Mean fluorescence Intensity
LM
hHIF2α-/-
CDAA 12 w
C
Serum IL-12
IL-12 ng/mL
p<0.001
p<0.001
Cont
CDAA 24w
LM
Cont
CDAA 24w
hHIF2α-/-

Figure 7

A

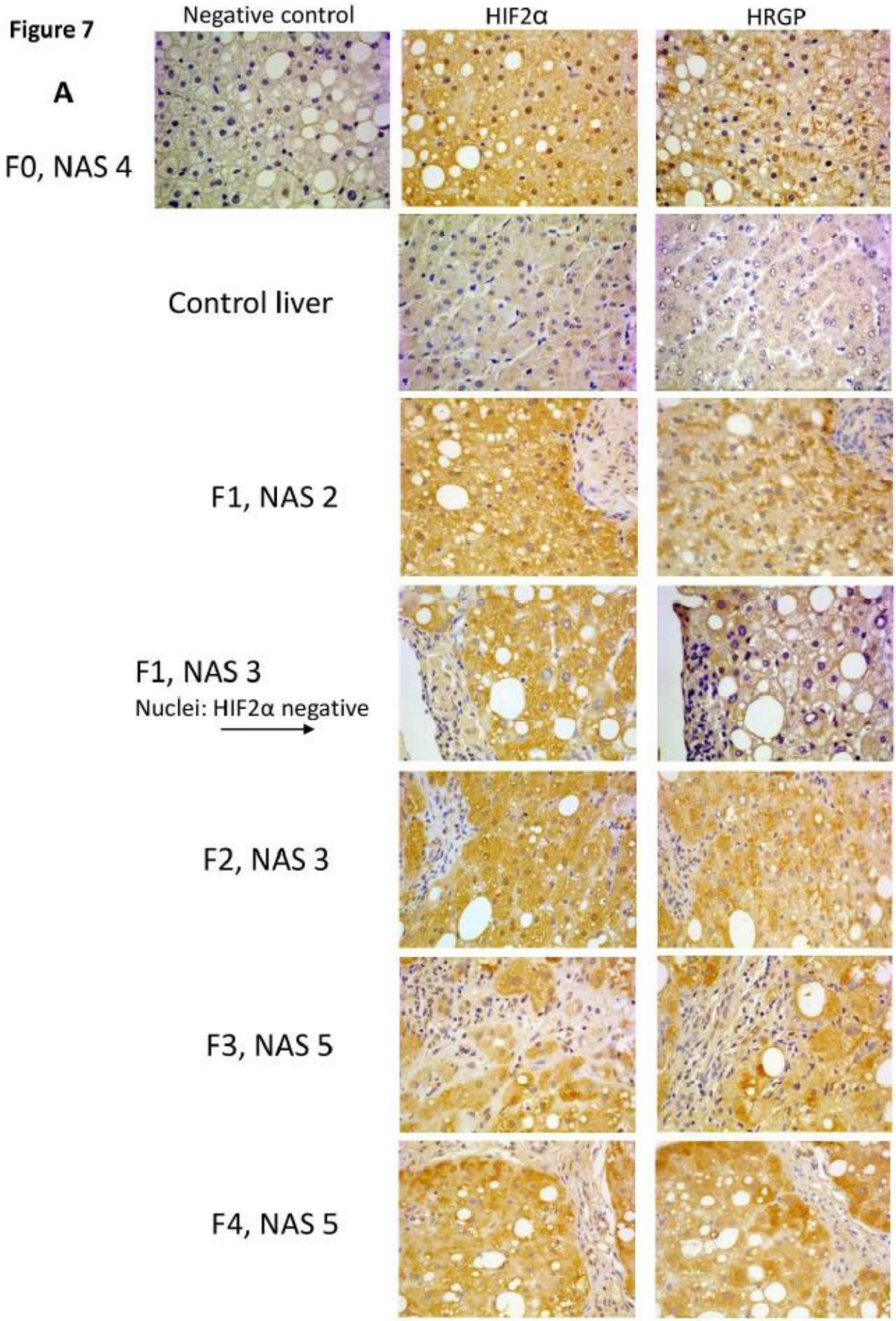
Negative control
HIF2α
HRGP
F0, NAS 4
Control liver
F1, NAS 2
F1, NAS 3
Nuclei: HIF2α negative
F2, NAS 3
F3, NAS 5
F4, NAS 5

Figure 7

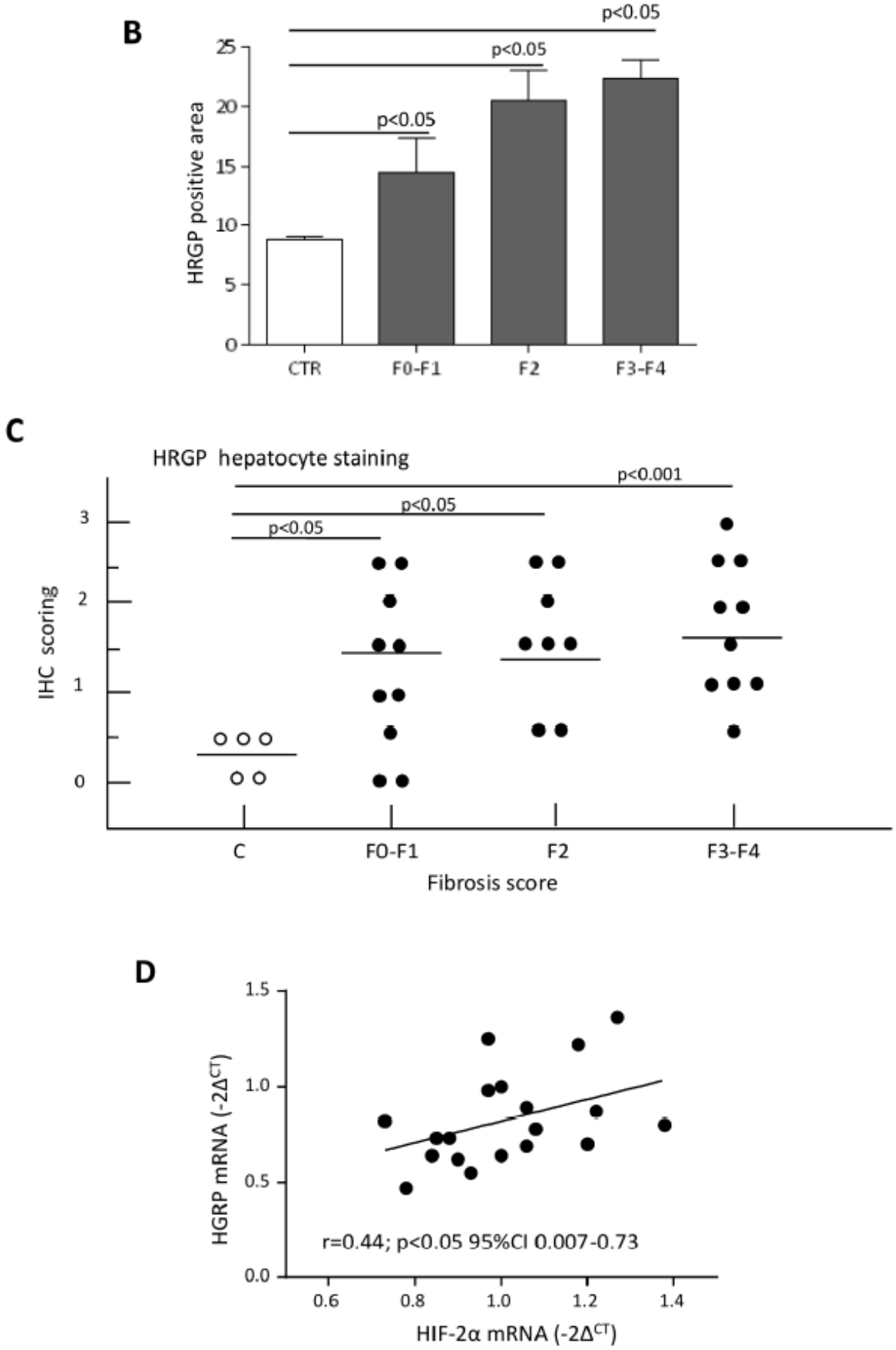
B
p<0.05
p<0.05
p<0.05
HRGP positive area
25
20
15
10
5
0
CTR
F0-F1
F2
F3-F4
C
HRGP hepatocyte staining
p<0.001
p<0.05
p<0.05
IHC scoring
3
2
1
0
C
F0-F1
F2
F3-F4
Fibrosis score
D
HGRP mRNA (-2Δ^CT)
1.5
1.0
0.5
0.0
r=0.44; p<0.05 95%CI 0.007-0.73
0.6
0.8
1.0
1.2
1.4
HIF-2α mRNA (-2Δ^CT)

Hypoxia-inducible factor 2α drives nonalcoholic fatty liver progression by triggering hepatocyte release of histidine rich glycoprotein

Elisabetta Morello[1]*, **Salvatore Sutti**[2,3]*, Beatrice Foglia[1], Stefania Cannito[1], Erica Novo[1], Claudia Bocca[1], Martina Rajsky[1], Stefania Bruzzì[3], Maria Lorena Abate[2], Chiara Rosso[2], Cristina Bozzola[3] Ezio David[4], Elisabetta Bugianesi[2], Emanuele Albano[3], Maurizio Parola[1§]

[1]Dept. Clinical and Biological Sciences, University of Torino, Italy.

[2]Dept. Medical Sciences, University of Torino, Italy.

[3]Dept. Health Sciences and Interdisciplinary Research Center for Autoimmune Diseases, University Amedeo Avogadro of East Piedmont, Novara, Italy.

[4]Pathology Unit, S. Giovanni Battista Hospital, Torino.

Table of contents.

Supplementary material and methods

Materials:

Enhanced chemiluminescence (ECL) reagents and nitrocellulose membranes (Hybond-C extra were from Amersham Pharmacia Biotech Inc. (Piscataway, NJ, USA). Polyclonal antibody against HIF-2α (NB100-122) was from Novus Biologicals (Cambridge, UK); GAPDH (sc-20357) was from Santa Cruz Biotechnology (Santa Cruz, CA, USA); mouse HRG (AF1905) was from R&D systems (Minneapolis, MN, USA) human HRG used for Western Blot detection (ab67807) was from Abcam (Cambridge, UK) and human HRG for immunohistochemistry experiments (HPA050269) was from Sigma (Sigma-Aldrich, St. Louis, MO, USA). Monoclonal antibodies for α-tubulin (T6074) and β-actin (A5441) were from Sigma (Sigma Aldrich Spa, Milan, Italy). Monoclonal antibodies against F4/80 for immunohistochemistry (14/4801/82) was from eBioscences (Affymetrix, St Clara, CA, USA) and α-SMA (M0851) was from DAKO (Agilent, St Clara, CA, USA). Lipofectamine 2000 (Invitrogen-Life Technologies), Plasmid DNA purification NucleoBond XtraMIDI (Macherey-Nagel, Germany), pCMV6-Entry vectors (Origene, Rockville, MD). RNA interference experiments to knockdown HIF-2α expression in HepG2 cells were performed using siRNA duplex (Qiagen Italia, Milano, Italy).

Immunohistochemistry, Sirius Red staining and histomorphometric analysis:

Paraffin-embedded human liver biopsies and/or murine liver specimens used in this study were immuno-stained as previously reported (1,2), and more details are reported in using polyclonal anti-HIF-2α antibody (dil. 1:100 v/v), polyclonal anti-HRGP antibody (dil. 1:50, v/v), monoclonal anti-α-SMA antibody (dil. 1:400, v/v) or F4-80 monocloclonal antibodies (dilution 1:1000, v/v). Collagen deposition was evidenced by Picro-Sirius Red staining as previously described, (30,31) and quantification of fibrosis in the murine liver was performed by histo-morphometric analysis using a digital camera and a bright field microscope to collect images that were then analyzed by employing the ImageJ software. (3) Hematoxilin/eosin stained mice liver sections were scored blind for steatosis and lobular inflammation. (4)

In vitro experiments and cell culture conditions:

In this study HepG2 cells (American Type Culture Collection, USA) were used and maintained in Dulbecco's modified Eagle's medium supplemented with 10% fetal-bovine serum, 100 U/ml penicillin, 100 µg/ml streptomycin and 25 µg/ml amphotericin-B, as previously reported. (1) In order to evaluate the HRGP protein levels under hypoxia condition, normal HepG2 cells were incubated in strictly controlled hypoxic conditions (3% O2) up to 72 hours.

The pCMV6-based mammalian expression vectors, empty (used as a control) and encoding HIF-2α (OriGene, Rockville, MD), were used in order to generate and select HepG2 cells stably overexpressing HIRF-2α. (28) HepG2 cells were seeded and then transfected 24 hr later with 10 µg of each vector using Lipofectamine 2000 (Invitrogen, Carlsbad, CA). HIF-2α expression of the generated stable transfectants was carefully characterized, after which the cell lines carrying the

empty vector (EV) and overexpressing HIF-2α (HepG2 Hif-2α) were then used for the experiment described.

RNA interference experiments to knockdown HIF-2α expression in HepG2 cells were performed using siRNA duplex as previously described [1]. The following target sequence was used:

-HIF-2α: 5′-CCCGGATAGACTTATTGCCAA-3′.

The siRNA and related non-silencing controls were transfected in HepG2 cells with lipofectamine 2000 transfection reagent according to manufacturer's instructions up to 72 hrs. Transfected cells in fresh medium were then exposed for further 48 hrs to the desired experimental conditions and then harvested for sample preparation.

Western blot analysis:

Total cell lysates, obtained as previously described, (1,3) were subjected to sodium dodecyl sulfate-polyacrylamide gel-electrophoresis on 12%, 10% or 7.5% acrylamide gels, incubated with desired primary antibodies, then with peroxidase-conjugated anti-mouse or anti-rabbit immunoglobulins in Tris-buffered saline-Tween containing 2% (w/v) non-fat dry milk and finally developed with the ECL reagents according to manufacturer’s instructions. Sample loading was evaluated by reblotting the same membrane with antibodies raised against GAPDH, α-tubulin and β-actin.

Supplementary Tables

Supplementary Table 1

Clinical and biochemical characterization of NAFLD patients investigated.

	Demographic Data
Patients Number (Male/Female)	27 (15/12)
Age (Years)	48 (23-70)
BMI	30.2 (22.3-39.6)
	Biochemical Data
HOMA-IR (n.v. <3)	3.7 (0.8-14.1)
AST (U/L– n.v. 5–40)	33.5 (16-93)
ALT (U/L n.v. 5–40)	44.1 (9-82)
γ-GT (U/L n.v. 5–45)	54.0 (11-525)
Fasting Glucose (mg/dL n.v. <100)	94.6 (72-197)
	Histological Data
Steatosis score	2 (0-3)
Inflammation score	1 (0-2)
Ballooning score	1 (0-2)
Fibrosis score	2 (0-4)
NAS score	4 (1-6)

The values are expressed as median and inter-quartile range (IQR). For histological scores the range of variability is included.

BMI, body mass index; AST, alanine aminotransferase; ALT, aspartate aminotransferase; γ-GT, gamma-glutamyl transpeptidase; HOMA-IR, homeostatic model assessment-insulin resistance; ISI, insulin sensitivity index; n.v., normal value

Supplementary Table 2

Oligonucleotide sequences of primers used for Q-PCR**.**

Gene	Primers
HIF1-α (mouse)	(FW) 5- TCAAGTTCAGCAACGTGGAAG -3 (RV) 5- TATCGAGGCTGTGTCGACTG -3
HIF2-α (mouse)	(FW) 5- CTAAGTGGCCTGTGGGTGAT -3 (RV) 5- GTGTCTTGGAAGGCTTGCTC-3
VEGF-A (mouse)	(FW) 5- CAGGCTGCTGTAACGATGAA-3 (RV) 5- TTTCTTGCGCTTTCGTTTTT -3
TGF-β (mouse)	(FW) 5- GGACTCTCCACCTGCAAGAC -3 (RV) 5- GACTGGCGAGCCTTAGTTTG -3
αSMA (mouse)	(FW) 5- CTGACAGAGGCACCACTGAA -3 (RV) 5- CATCTCCAGAGTCCAGCACA -3
COL1A1 (mouse)	(FW) 5- GAGCGGAGAGTACTGGATCG -3 (RV) 5- GTTCGGGCTGATGTACCAGT -3
TIMP1 (mouse)	(FW) 5- ATTCAAGGCTGTGGGAAATG -3 (RV) 5- CTCAGAGTACGCCAGGGAAC -3
β-ACTIN (mouse)	(FW) 5-AGCCATGTACGTAGCCATCC -3 (RV) 5- CTCTCAGCTGTGGTGGTGAA -3
HIF2-α (human)	(FW) 5- CGCTAGACTCCGAGAACAT -3 (RV) 5- GGCTTGAACAGGGATTCAGT -3
β-ACTIN (human)	(FW) 5- AGAGCTACGAGCTGCCTGAC -3 (RV) 5- GGATGCCACAGGACTGGA -3
HRG (human)	(FW) 5- GCCCGAAAAACCTTGTCATA -3 (RV) 5- CTAGATCCATGGGGCTTGAA -3
CXCR4 (mouse)	(FW) 5- TGGAACCGATCAGTGTGAGT -3 (RV) 5- TTGCCGACTATGCCAGTCAA -3
CXCR4 (human)	(FW) 5- TCCATTCCTTTGCCTCTTTTGC -3 (RV) 5- ACGGAAACAGGGTTCCTTCAT -3
FASN (mouse)	(FW) 5- TGGGTTCTAGCCAGCAGAGT -3 (RV) 5- ACCACCAGAGACCGTTATGC -3
SREBP1 (mouse)	(FW) 5- GATCAAAGAGGAGCCAGTGC -3 (RV) 5- TAGATGGTGGCTGCTGAGTG -3
EPO (human)	(FW) 5- GAGCCCAGAAGGAAGCCATC -3 (RV) 5- GCGGAAAGTGTCAGCAGTGA -3

Supplementary Figures

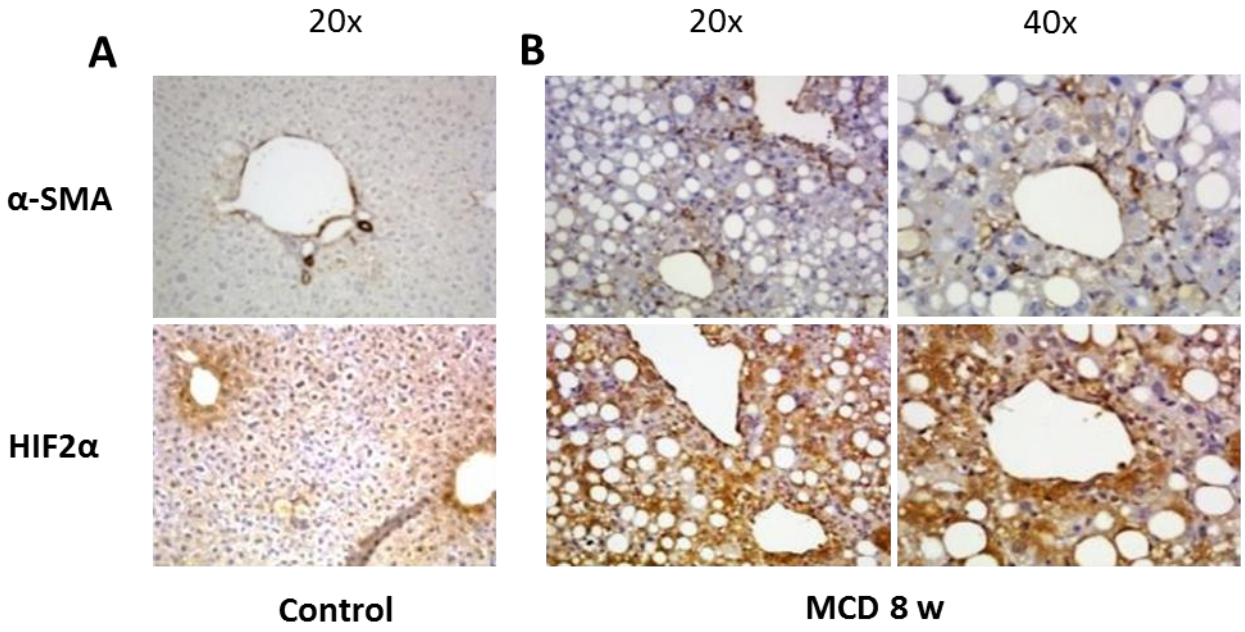

Morello E et al., Suppl. Figure 1A,B

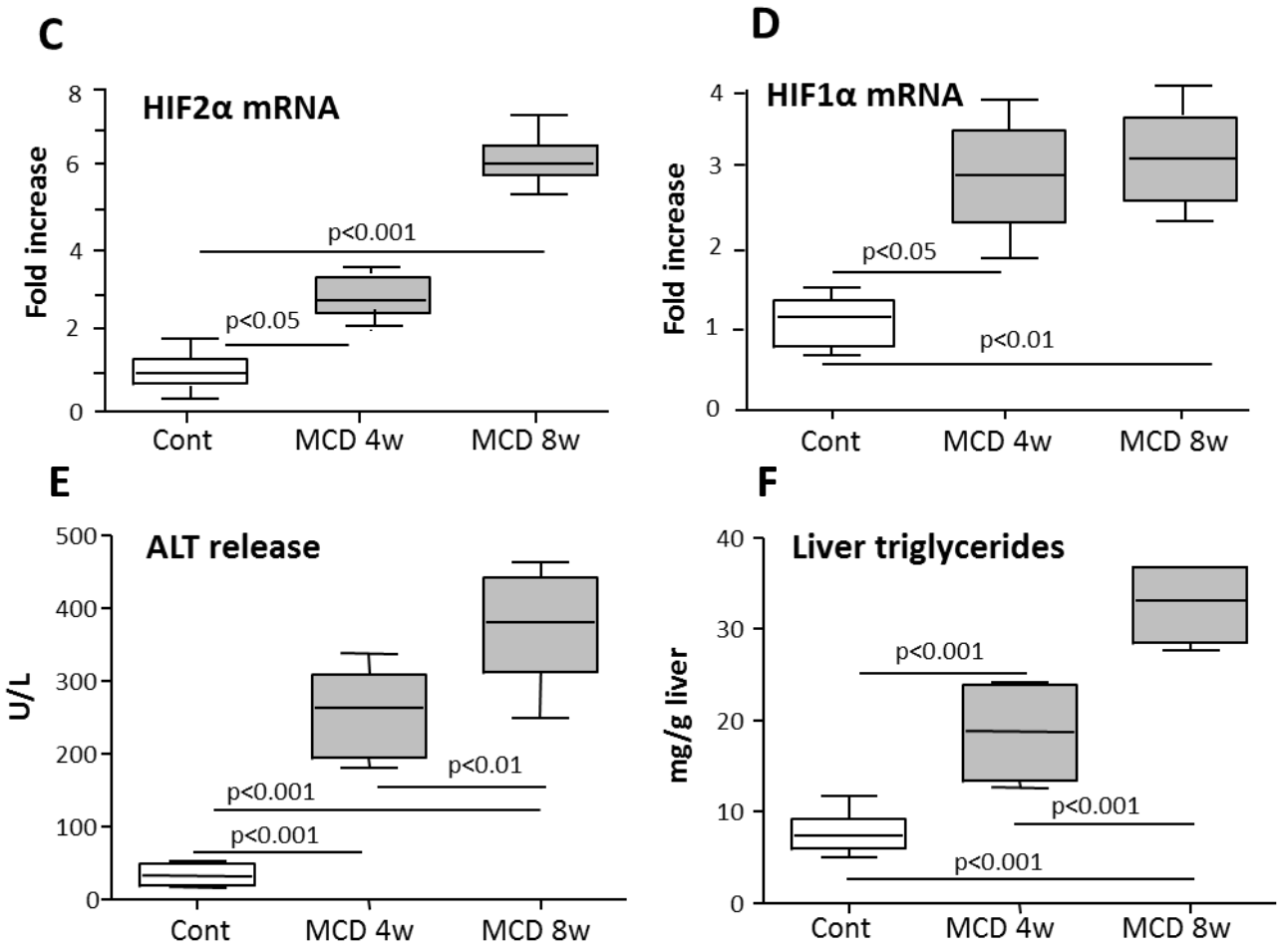

Morello et al. Suppl. Figure 1C-F

Suppl. Fig. 1. **Expression of HIF-2α in mice liver**. Immunohistochemistry analysis for HIF-2α and α-smooth muscle actin (α-SMA) in liver specimens from wild type mice fed with control (**A**) or MCD diet (8 weeks) (**B**). Original magnification as indicated. Liver expression of HIF-2α (**C**) and HIF-1α (**D**), evaluated by quantitative real-time PCR (Q-PCR) in MCD fed mice (4 and 8 weeks). Parenchymal injury and steatosis, estimated by measuring the circulating levels of alanine (ALT) **(E)** and hepatic TG content **(F)** are reported in MCD fed mice. The mRNA values are expressed as fold increase over control values after normalization to the β-actin gene expression. The data are means ± SD of 5-7 animals per group. Boxes include the values within 25th and 75th percentile, whereas horizontal bars represent the medians. The extremities of the vertical bars (10th-90th percentile) comprise 80% of the values. Statistical differences were assessed by one-way ANOVA test with Tukey's correction for multiple comparisons.

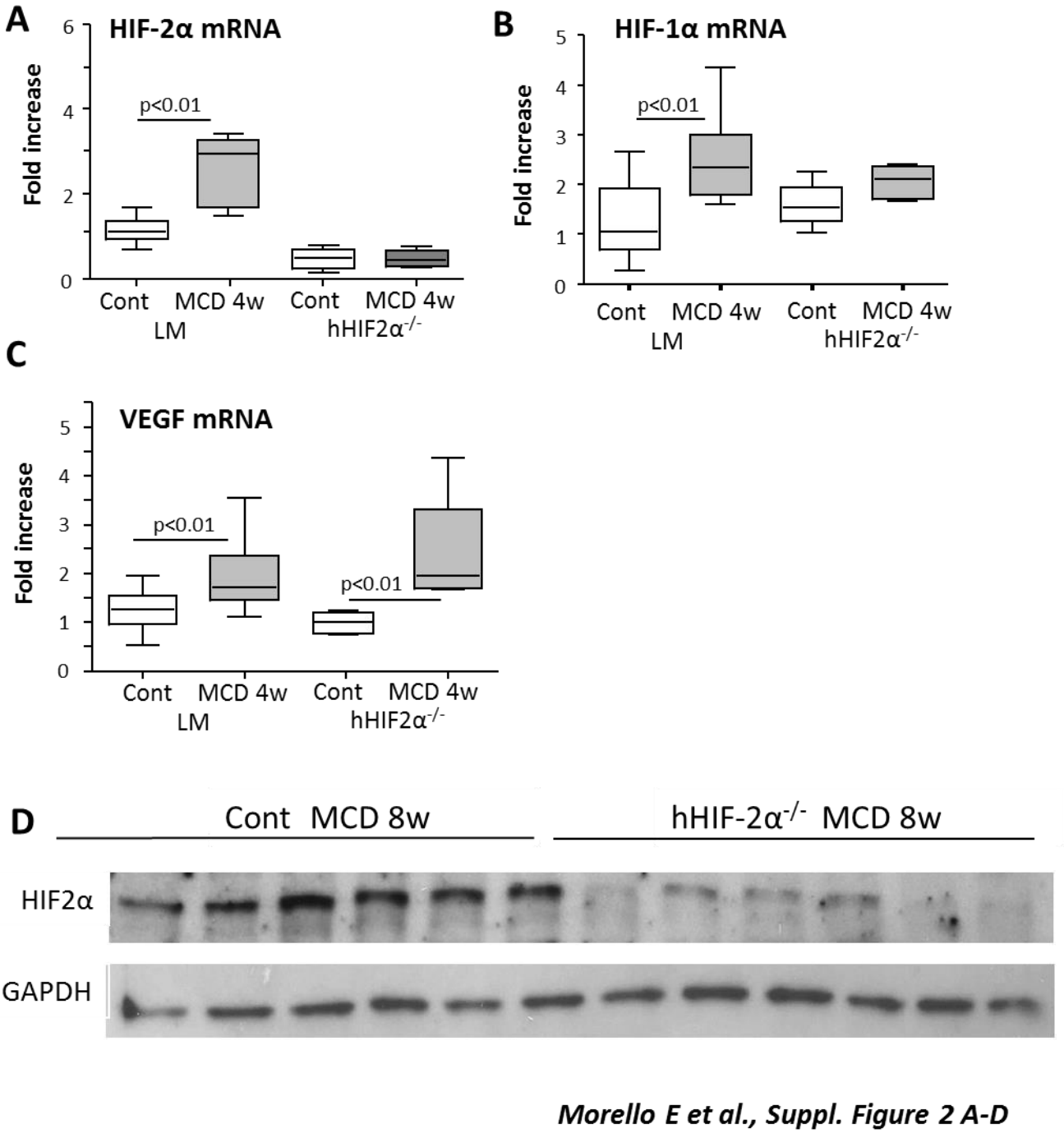

Suppl. Fig. 2. HIFs and VEGF gene expression in mice carrying hepatocyte-specific deletion of HIF-2α. Gene expression of HIF-2α (**A**), HIF-1α (**B**) and VEGF (**C**) evaluated by quantitative real-time PCR (Q-PCR) in livers of wild type littermates (LM) and hHIF2α$^{-/-}$ mice fed with the MCD diet for 4 weeks. The mRNA values are expressed as fold increase over control values after normalization to the β-actin gene expression. The data are means ± SD of 5-7 animals per group. Boxes include the values within 25th and 75th percentile, whereas horizontal bars represent the medians. The extremities of the vertical bars (10th-90th percentile) comprise 80% of the values. Statistical differences were assessed by one-way ANOVA test with Tukey's correction for multiple comparisons. Western blot analysis of HIF-2α protein levels was performed on total liver extracts obtained from either LM and hHIF2α $^{-/-}$ mice fed MCD diet for 8 weeks (**D**).

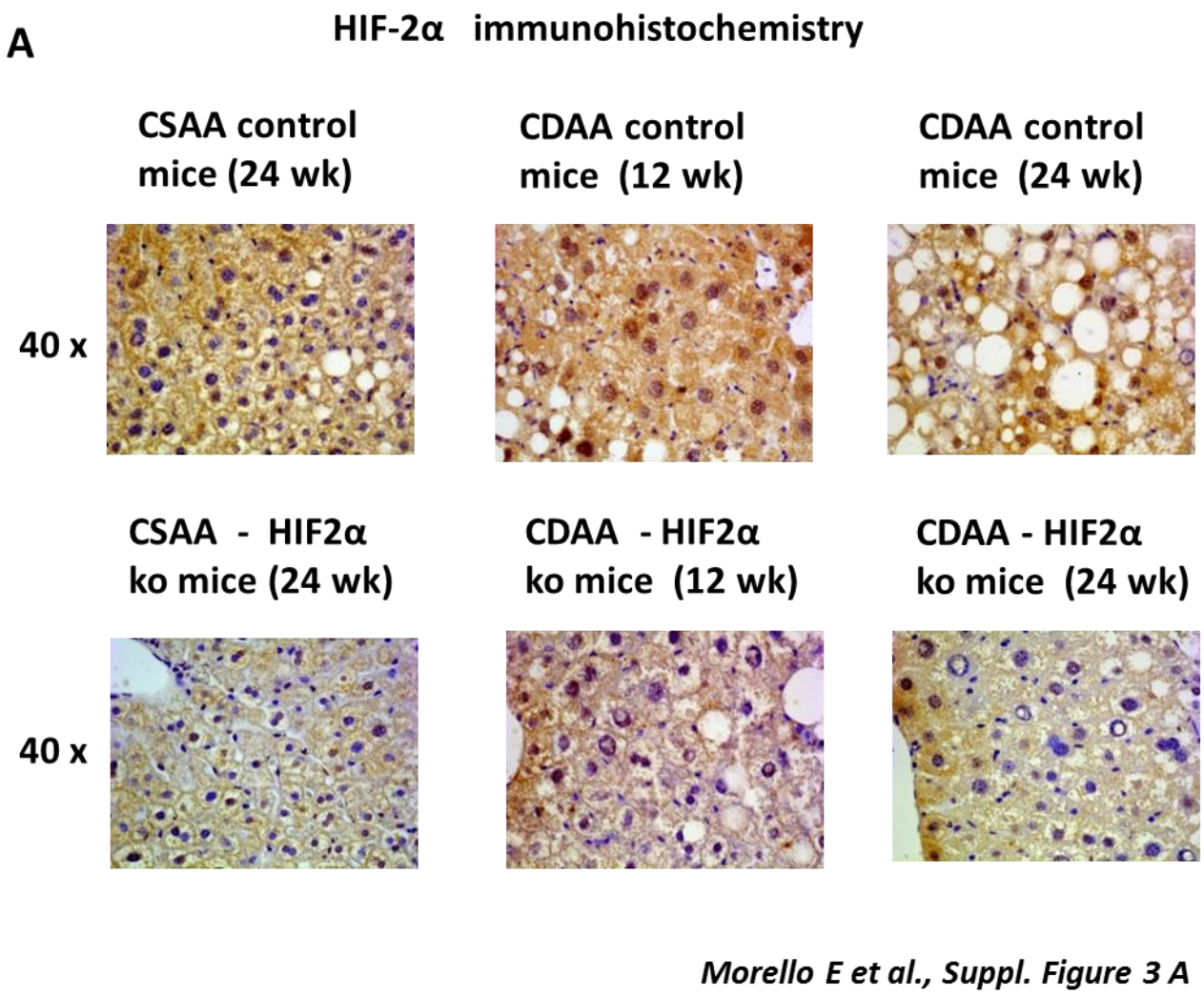

Suppl. Fig. 3. Expression of HIF-2α in mice liver. Immunohistochemistry analysis for HIF-2α in the livers of wild type littermates (LM) or hHIF-2α$^{-/-}$ CDAA or CSAA fed animals (12 and 24 weeks) (**A**). Original magnification as indicated.

Suppl. Figure 3

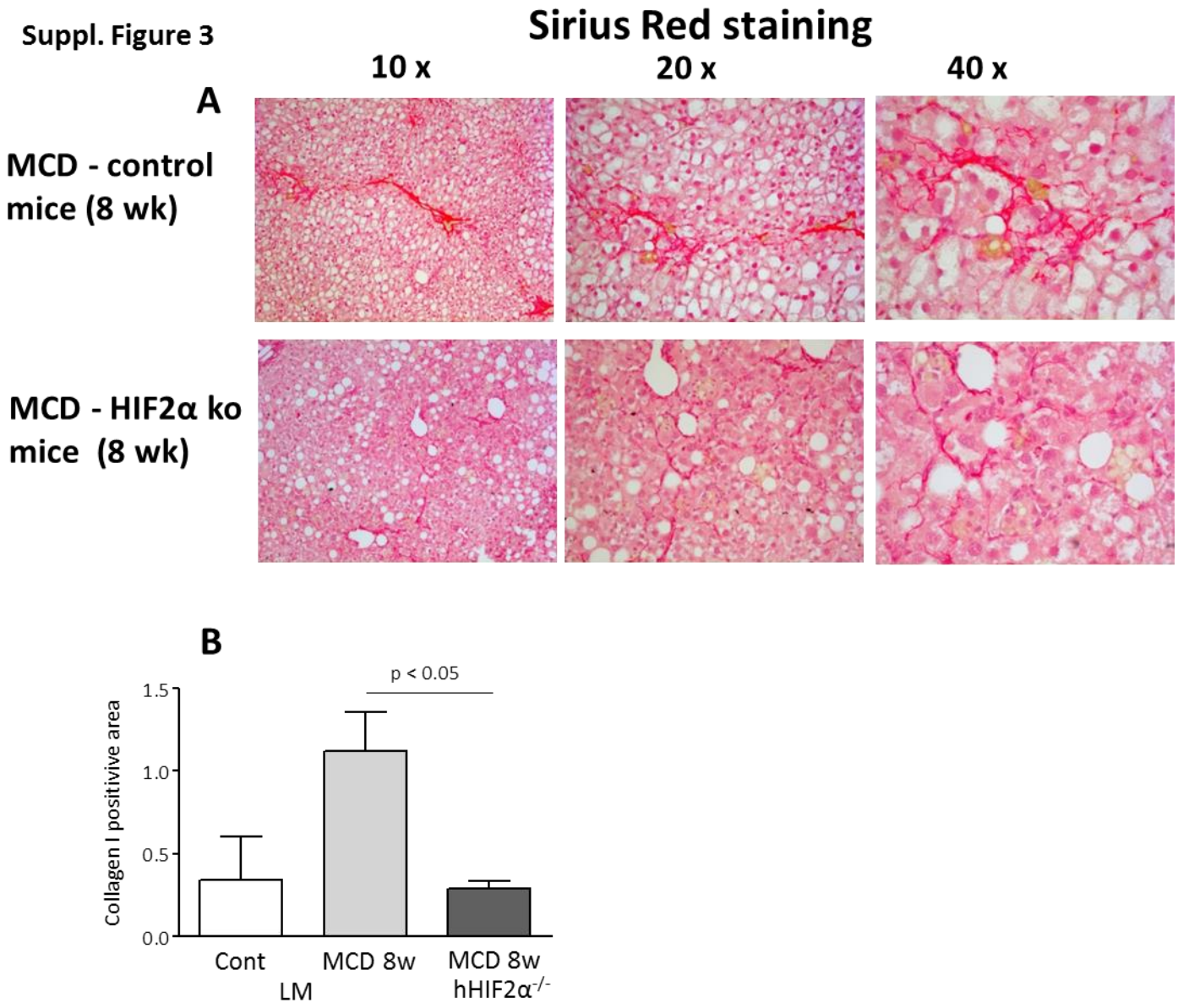

Morello E et al. Suppl. Figure 4 A,B

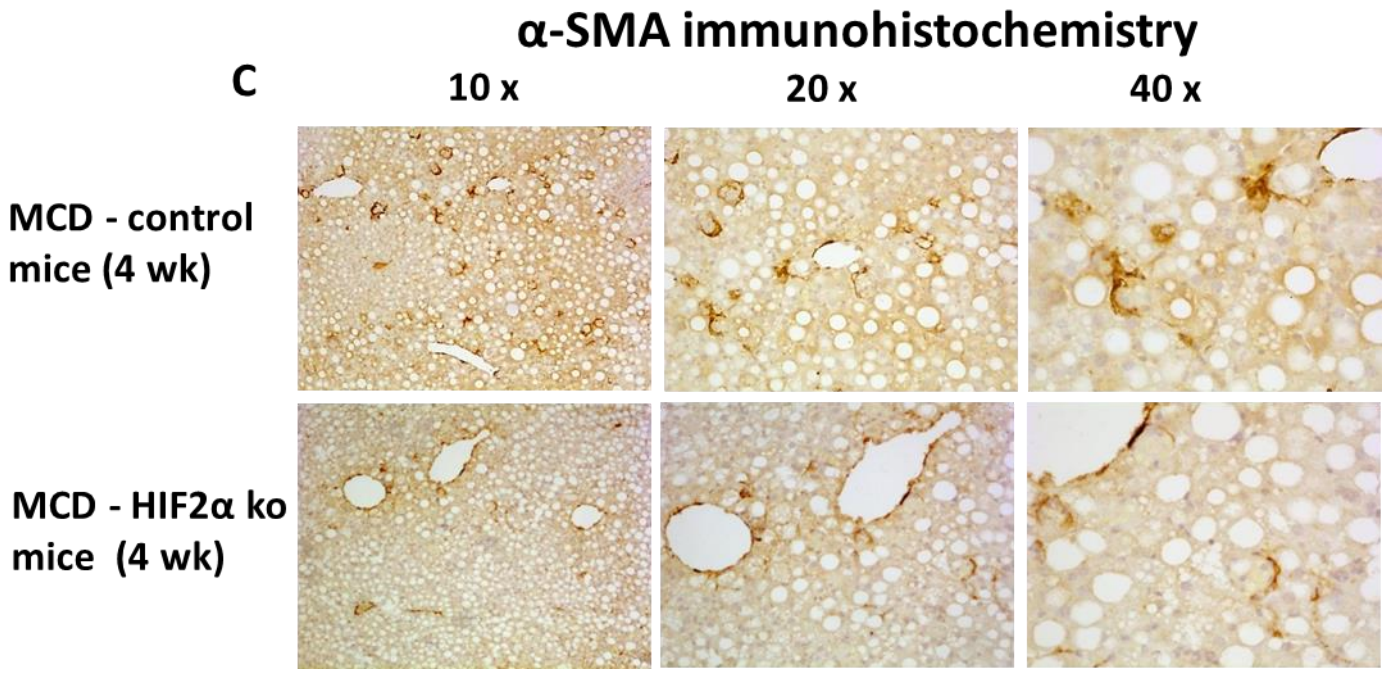

Morello E et al. Suppl. Figure 4 C

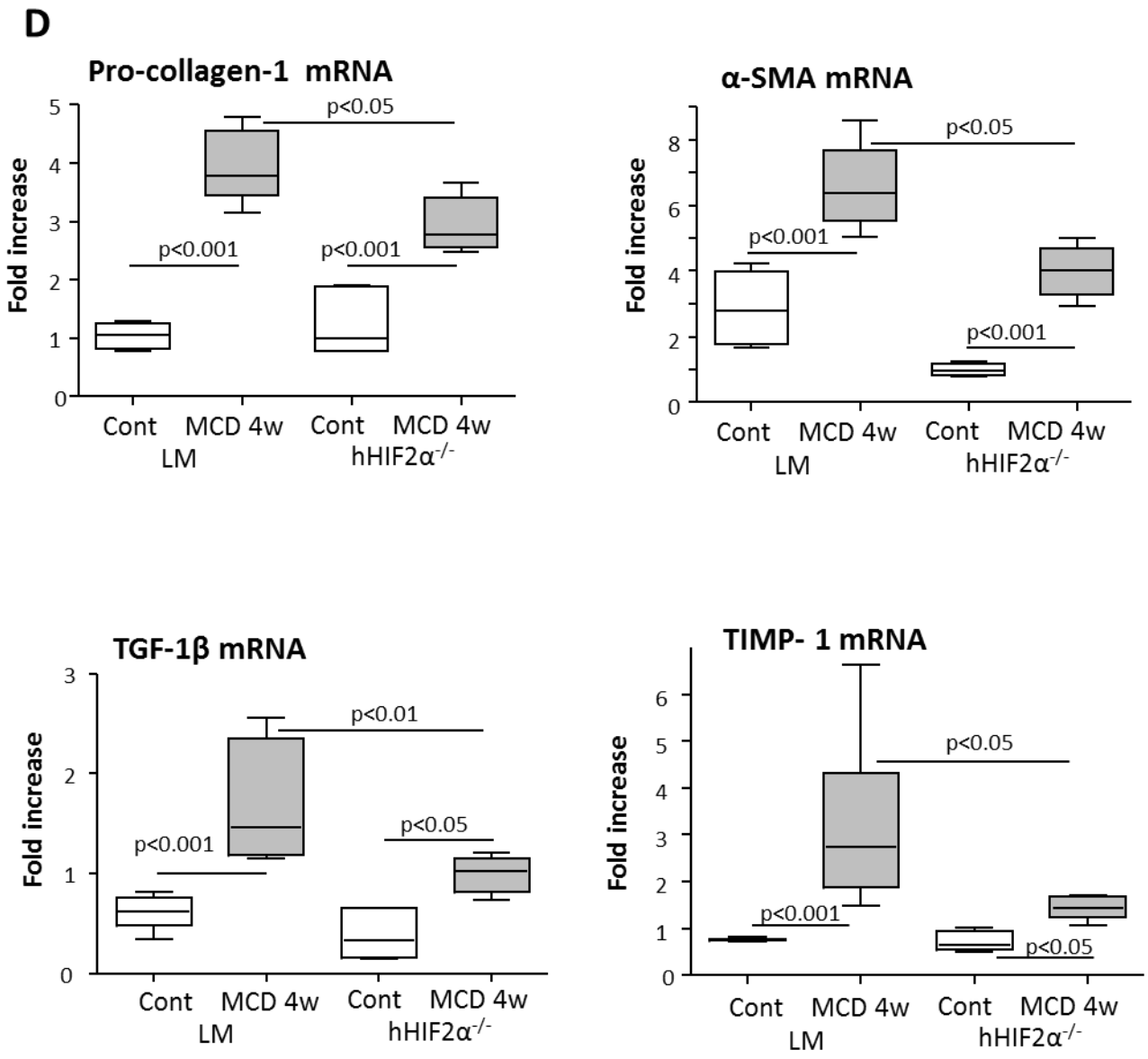

Morello E et al. Suppl. Figure 4 D

Suppl. Fig. 4 A-D. Effect on liver fibrosis of hepatocyte deletion of HIF-2α. hHIF-2$\alpha^{-/-}$ mice and wild type littermates (LM) were fed with MCD diet for 8 weeks. Liver fibrosis was morphologically evaluated by Sirius red staining (**A**). Original magnification as indicated. ImageJ software analysis was performed for Sirius red staining (**B**) to evaluate the amount of fibrosis. Immunohistochemistry for α-SMA (**C**) in the same animals. Data in graphs are expressed as means ± SEM. Analysis by quantitative real-time PCR (Q-PCR) of transcript levels of pro-fibrogenic genes pro-collagen 1A1, αSMA, TGFβ1 and TIMP1 in the different experimental groups (**D**). The mRNA values are expressed as fold increase over control values after normalization to the β-actin gene expression. The data are means ± SD of 6-7 animals per group. Boxes include the values within 25th and 75th percentile, whereas horizontal bars represent the medians. The extremities of the vertical bars (10th-90th percentile) comprise 80% of the values. Statistical differences were assessed by one-way ANOVA test with Tukey's correction for multiple comparisons.

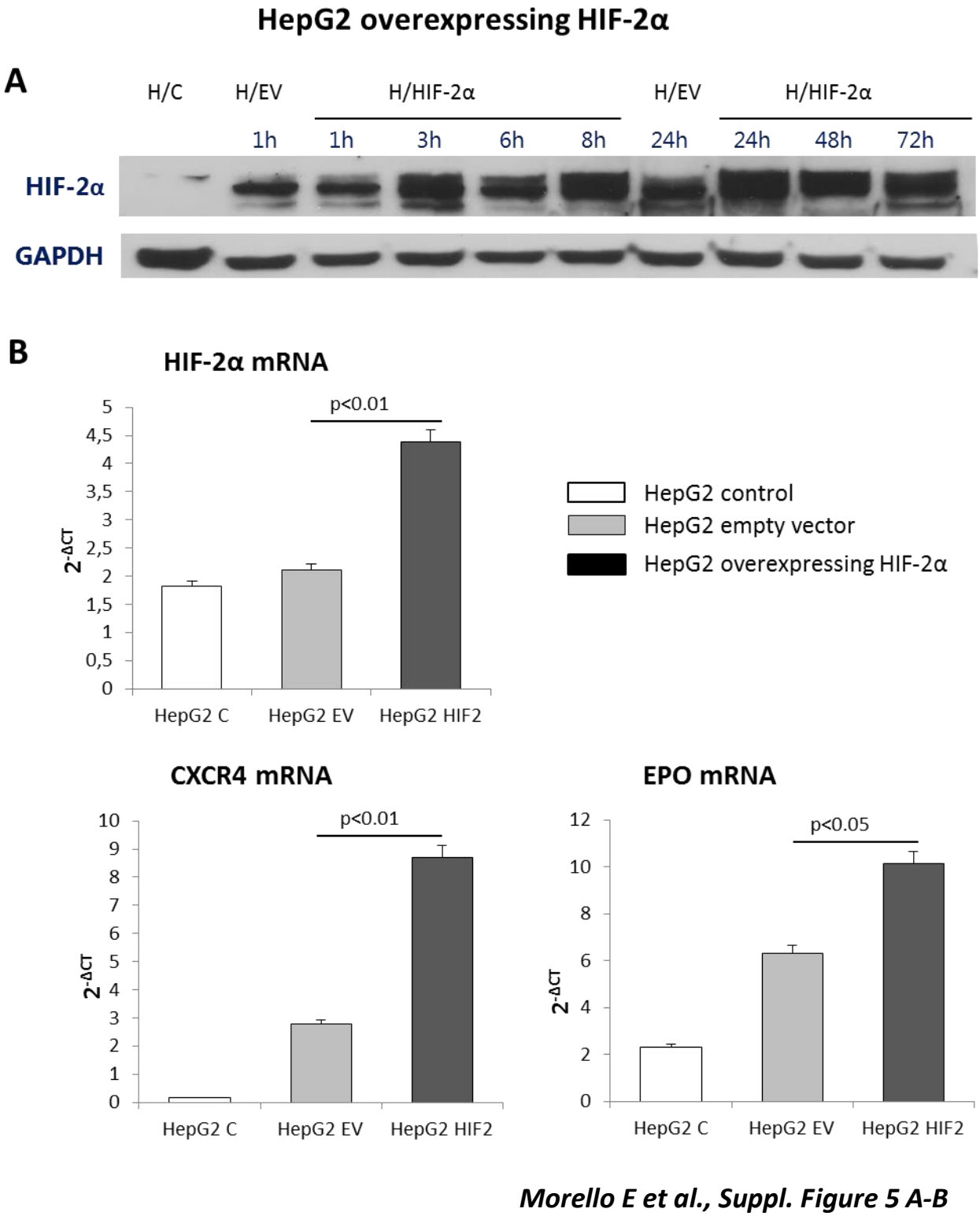

Morello E et al., Suppl. Figure 5 A-B

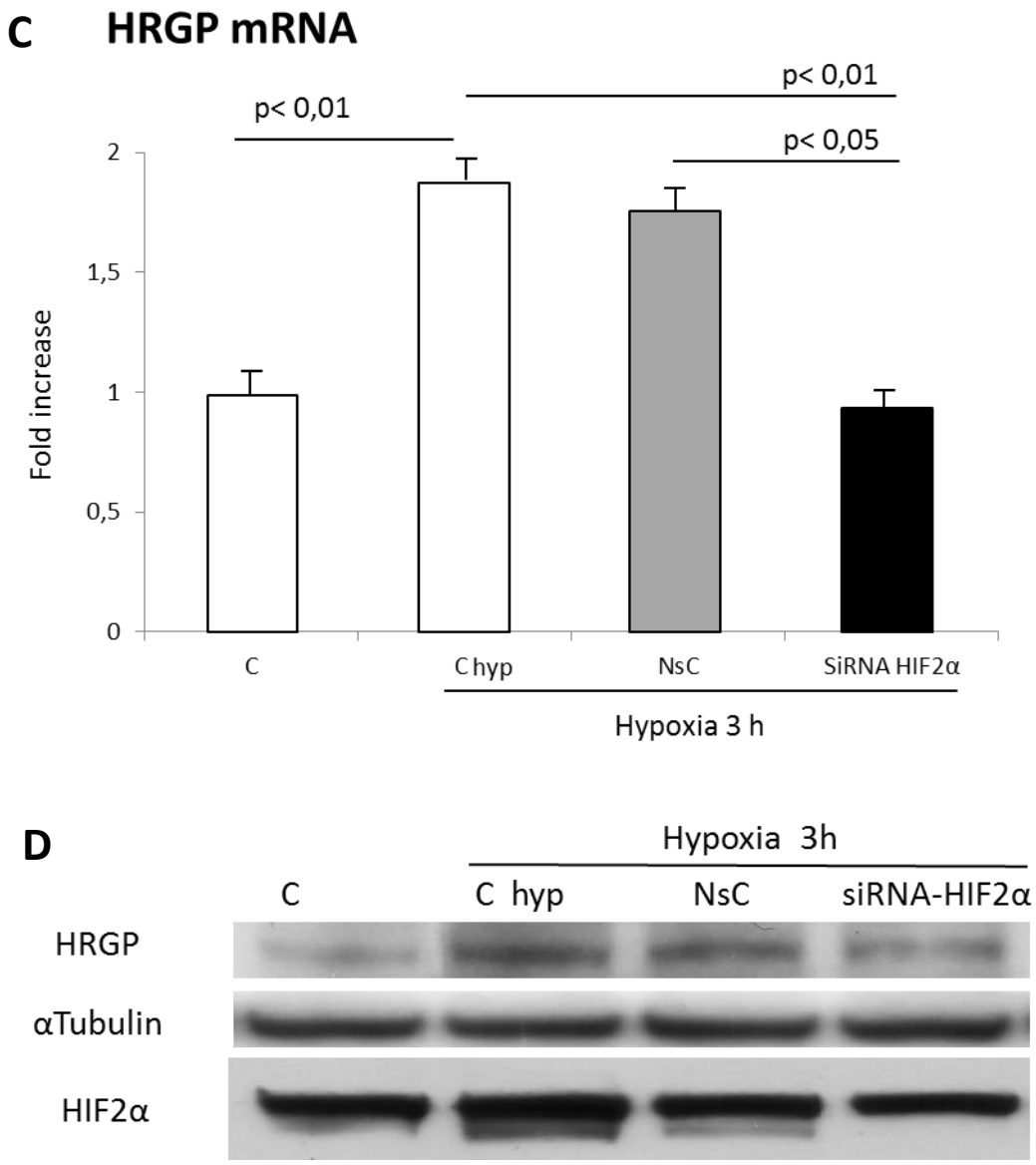

Morello E et al., Suppl. Figure 5 C

Suppl. Fig. 5. Direct relationships between HIF2α and HRGP expression. Western blotting analysis of HIF-2α levels in control HepG2 cells or HepG2 cells stably transfected to over-express HIF-2α exposed to hypoxic conditions (H/C: not transfected; H/EV: transfected with empty vector; H/HIF-2α: overexpressing HIF-2α) (**A**). Q-PCR analysis of HIF-2α and related targets transcript, including CXCR4 and erythropoietin (EPO) in control HepG2 cells (HepG2 C: not transfected; EV: transfected with empty vector) or HepG2 cells stably transfected to over-express HIF-2α (**B**). Q-PCR **(C)** and WB analysis **(D)** of HRGP transcript and protein levels in untreated HepG2 in normoxic conditions (C) or in HepG2 exposed for three hours to hypoxic conditions only (C hyp) as previously described (1) or in HepG2 exposed to hypoxia following silencing for HIF-2α with a specific siRNA (siRNA-HIF2α) or treatment with a non-silencing siRNA (NsC) **(C,D)**. WB analysis is offered also for HIF2α protein levels **(D)**. Data in graphs are expressed as means ± SEM. Statistical differences were assessed by one-way ANOVA test with Tukey's correction for multiple comparisons.

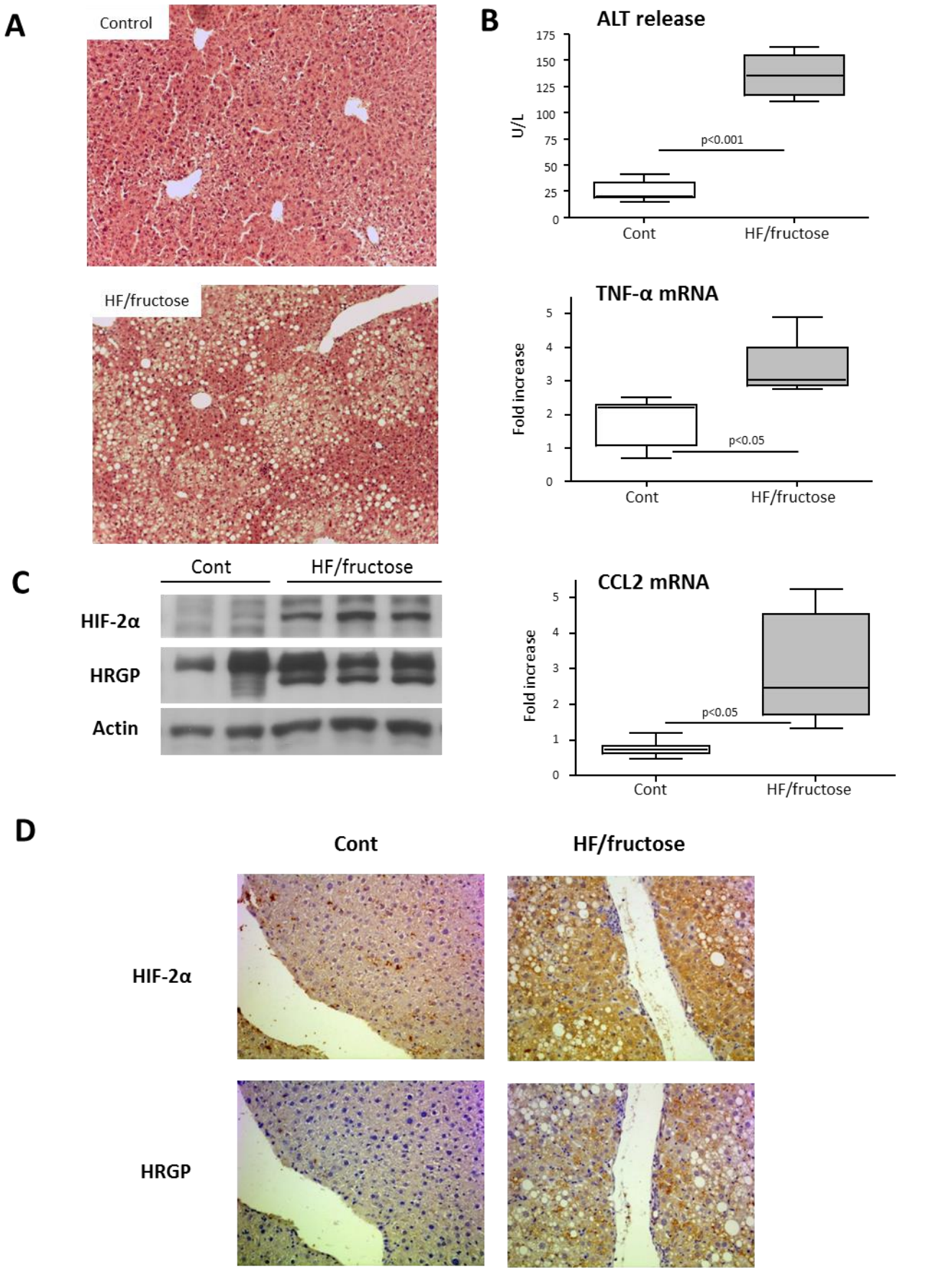

Morello E et al., Suppl. Figure 6 A-D

Suppl. Fig. 6. HIF-2α and HRGP expression in mice fed on High Fat / Fructose diet. C57BL/6 wild type mice were fed for 24 weeks with an high fat diet (58% of energy derived from fat, 18% from protein, and 24% from carbohydrates; 5.6 kcal/g) (Envigo RMS, S Pietro al Natisone, Italy) supplemented with 15% fructose (wt/v) in the drinking water. Liver morphology in mice exposed to HF/fructose mice diet or related control diet was evaluated by hematoxylin/eosin staining (magnification 10X) (**A**). Parenchymal injury was evaluated by measuring the serum levels of alanine (ALT) and pro-inflammatory citokynes mRNA levels (**B**). Elevation of both HIF-2α and HRGP protein levels was detected by Western blotting (**C**) and immune-histochemistry (IHC) analyses (magnification 20X) (**D**). The mRNA values are expressed as fold increase over control values after normalization to the β-actin gene expression and are means ± SD of 6-8 animals per group. The boxes include the values within 25^{th} and 75^{th} percentile, while the horizontal bars represent the medians. The extremities of the vertical bars (10^{th}-90^{th} percentile) comprise the eighty percent of the values. Statistical differences were assessed by one-way ANOVA test with Tukey's correction for multiple comparisons.

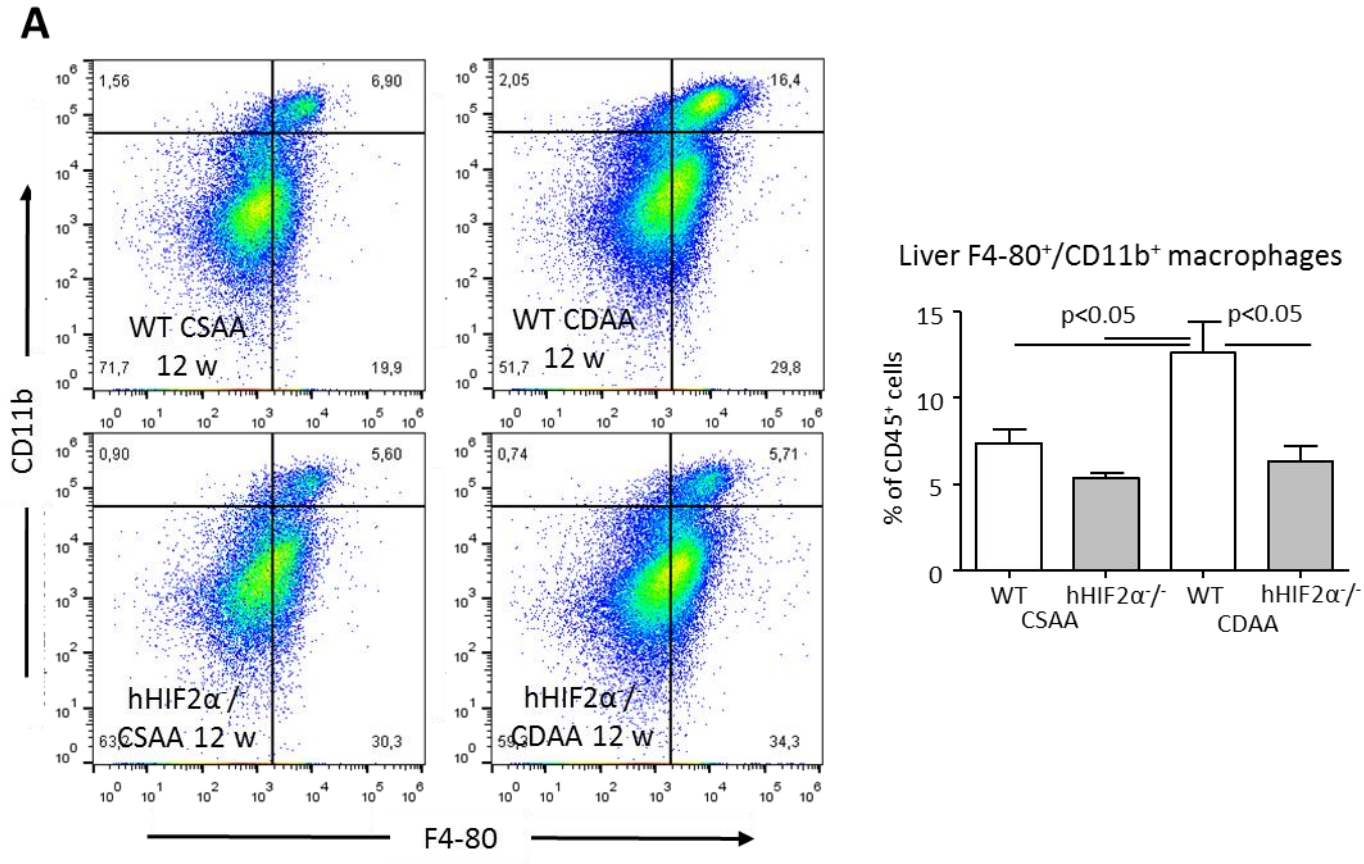

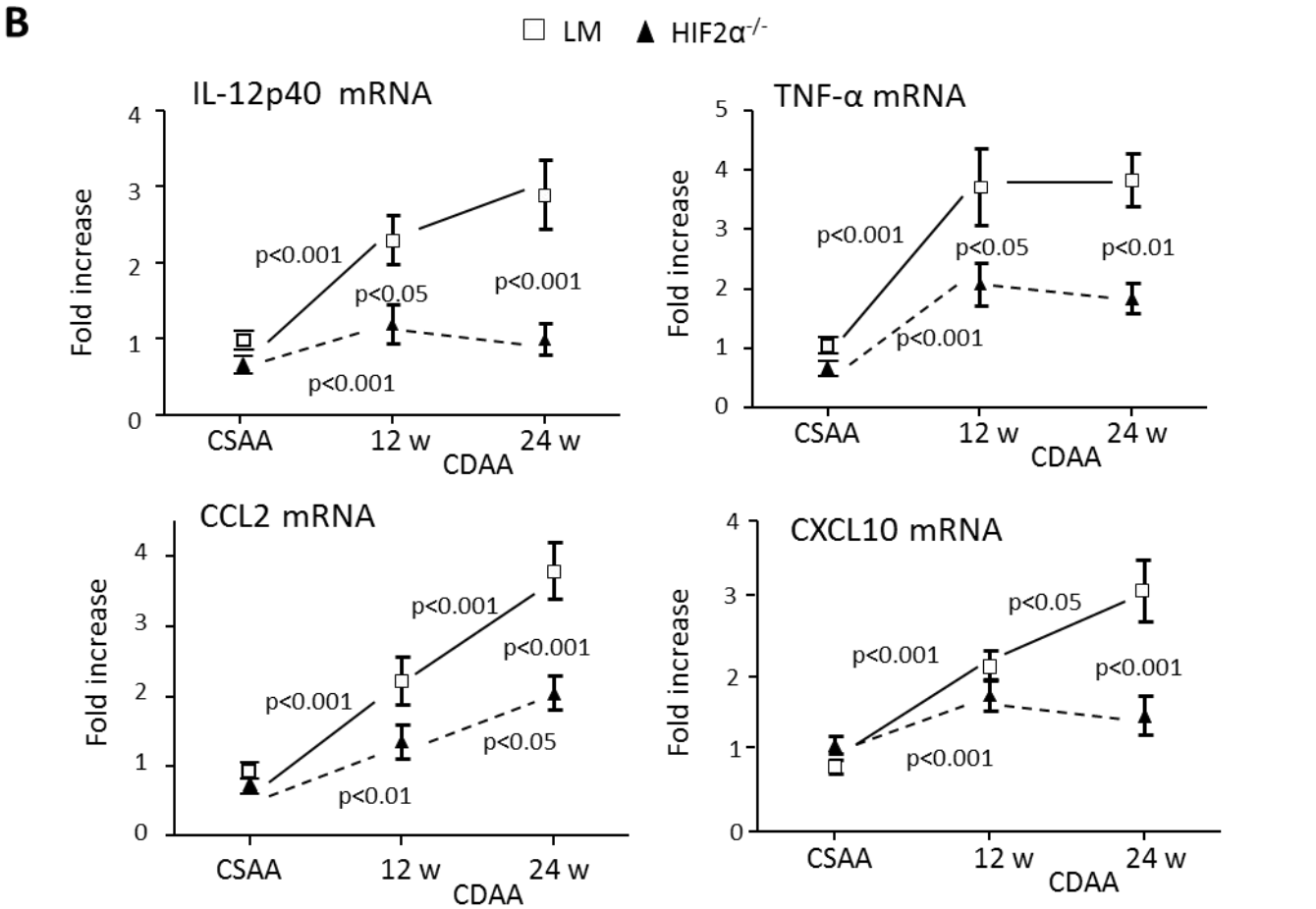

Morello E et al., Suppl. Figure 7 A-B

Suppl. Fig. 7. HIF2α-deficiency regulates macrophage infiltration. Hepatic myeloid cells were isolated from livers of either hHIF-2α$^{-/-}$ mice and wild type littermates (LM) fed with the CDAA diet analyzed by flow cytometry for Cd11b expression in CD45/F4-80-positive liver macrophages (**A**). Liver expression of inflammatory markers IL-12p40, TNF-α, CCL2 and CXCL10 was evaluated by quantitative real-time PCR (Q-PCR). The mRNA values are expressed as fold increase over control values after normalization to the β-actin gene expression and are means ± SD of 6-8 animals per group (**B**). Statistical differences were assessed by one-way ANOVA test with Tukey's correction for multiple comparisons.

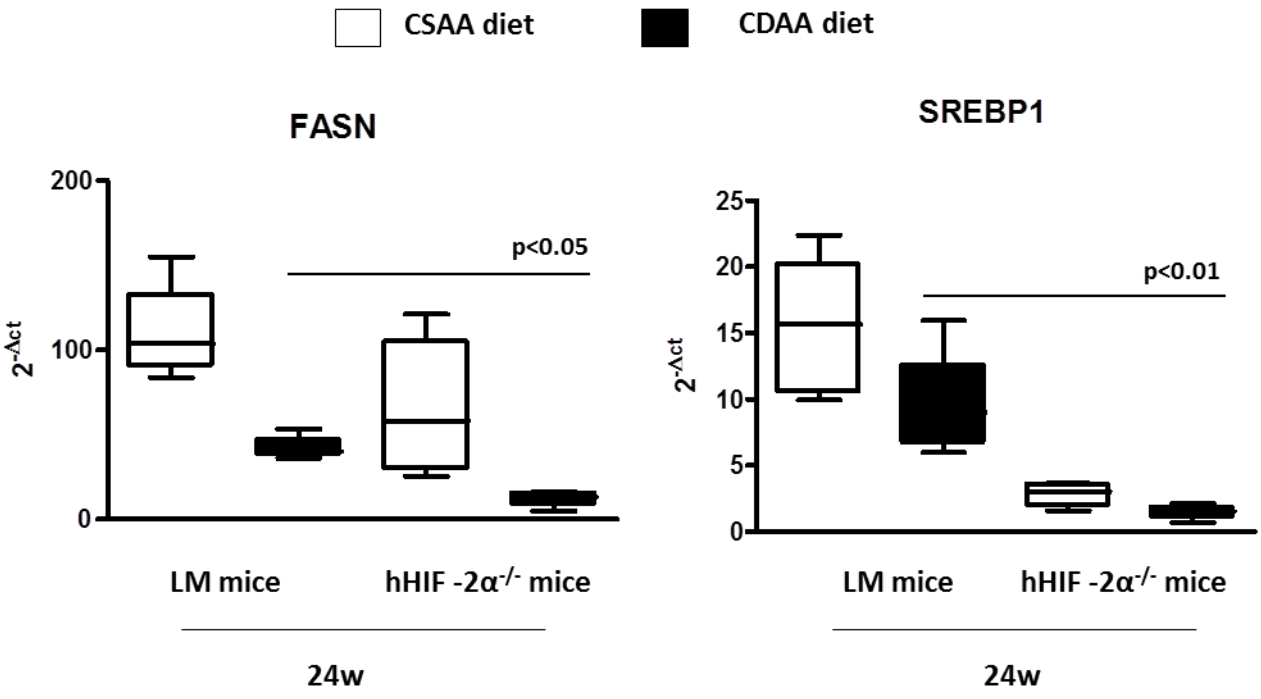

Suppl. Fig. 8. HIF-2α modulates lipid homeostatic genes in the liver. qPCR analysis of sterol regulatory element binding factor -1 (SREBP1) and fatty acid synthase (FASN) in livers from hHIF-2α-/- mice vs related control littermates exposed to CDAA or CSAA diet. The mRNA values are expressed after normalization to the β-actin gene expression and are means ± SD of 6-8 animals per group. The boxes include the values within 25th and 75th percentile, while the horizontal bars represent the medians. The extremities of the vertical bars (10th-90th percentile) comprise the eighty percent of the values. Statistical differences were assessed by one-way ANOVA test with Tukey's correction for multiple comparisons.

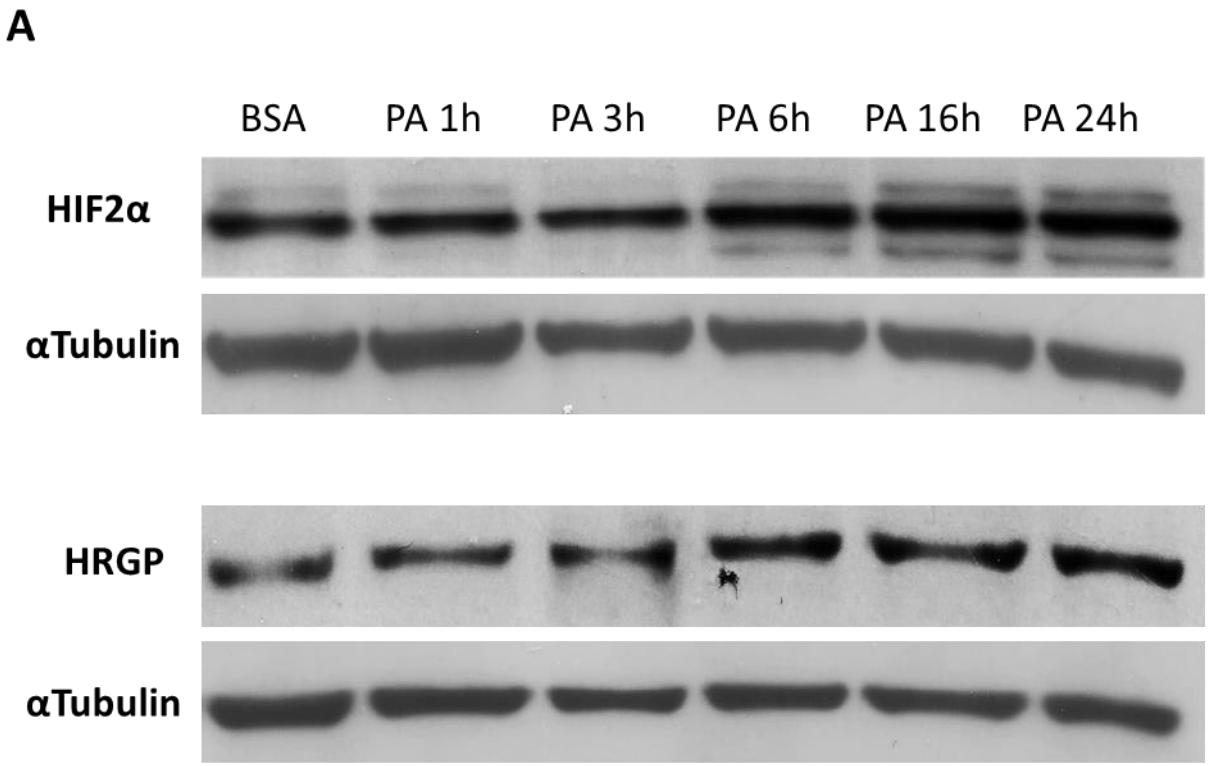

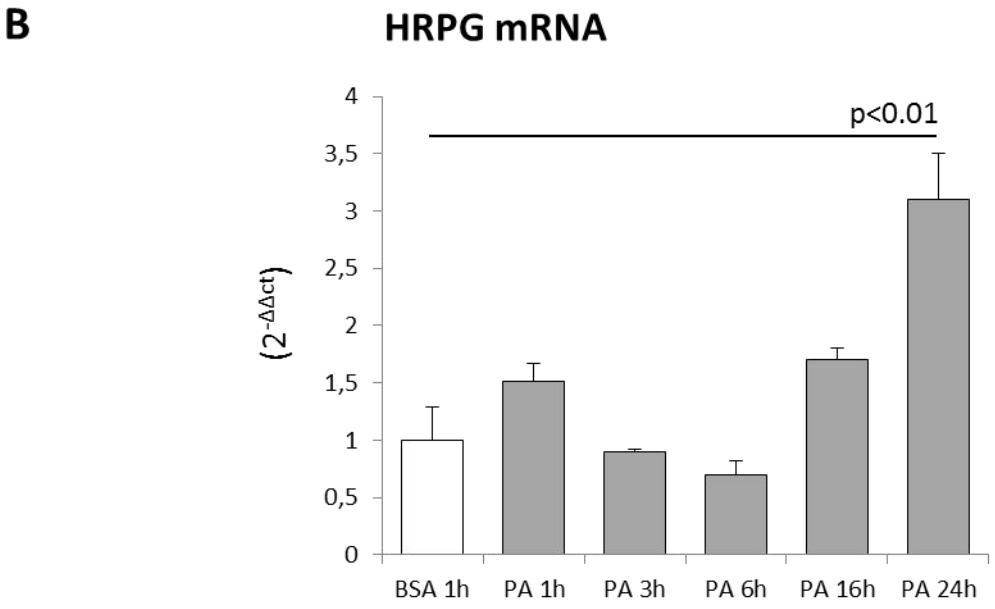

Morello E et al., Suppl. Figure 9 A - B

Suppl. Fig. 9. Murine hepatocytes treated with palmitic acid. Western blotting analysis of both HIF-2α and HRGP levels in AML12 cell line treated with palmitic acid 0,25mM up to 24hrs (**A**). Q-PCR analysis of HRGP in AML12 hepatocytes treated with palmitic acid 0,25mM up to 24hrs (**B**). Data in graphs are expressed as means ± SEM. Statistical differences were assessed by one-way ANOVA test with Tukey's correction for multiple comparisons.

References for Supplementary Material

1. Cannito S, Turato C, Paternostro C, Biasiolo A, Colombatto S, Cambieri I, et al. Hypoxia up-regulates SERPINB3 through HIF-2α in human liver cancer cells. Oncotarget 2015; 6:2206-2221.

2. Novo, E, Busletta C, Valfrè di Bonzo L, Povero D, Paternostro C, Mareschi K, et al. Intracellular reactive oxygen species are required for directional migration of resident and bone marrow-derived hepatic pro-fibrogenic cells. J Hepatol 2011;54:964-974.

3. Novo E, Villano G, Turato C, Cannito S, Paternostro C, Busletta C, et al. SerpinB3 promotes pro-fibrogenic responses in activated hepatic stellate cells. Scientific Reports 2017;7(1):3420.

4. Kleiner DE, Brunt EM, Van Natta M, Behling C, Contos MJ, Cummings OW, et al. Design and validation of a histological scoring system for nonalcoholic fatty liver disease. Hepatology 2005;41:1313-1321.